# FEASIBILITY OF UTILIZING INTEGRATED GASIFICATION COMBINED CYCLE (IGCC) BYPRODUCTS FOR NOVEL MATERIALS DEVELOMENT

## FINAL REPORT

By:

Frederick Douglas
COSMOS Technologies, Inc.
Yoginder P. Chugh
Southern Illinois University
Carbondale, Illinois

For:

National Energy Technology Laboratory
Pittsburgh, PA
DOE Cooperative Agreement: DE-AF26-04NT40752

August 2006

# TABLE OF CONTENTS

## LIST OF FIGURES

# LIST OF TABLES

# DISCLAIMER

# ACKNOWLEDGEMENTS

The authors sincerely acknowledge the financial support of the National Energy Technology Laboratory of the U.S. Department of Energy. In addition, thanks are also expressed to several individuals and organizations that supported in significant ways to complete this investigation. Particular thanks are due to the following.

- William Aljoe for his technical support and constructive comments during this study.
- A Utility Company for providing samples of IGCC byproducts.
- Mr. Phil Amick of Conoco-Phillips for technical discussions and input as needed.
- Ferro Corporation for performing analytical studies and providing input on the potential to develop pigments and frit from byproducts.
- Several rock wool manufacturing companies for evaluating the characterization data of the IGCC byproduct frit material and commenting on the feasibility of producing rock wool from this material.
- Professor Carlo G. Pantano and research assistant, Rob Schaut, of the Pennsylvania State University Materials Research Institute, for studies related to the glass making potential of IGCC FRIT material.
- Dr. Willy Balaba, an independent consultant, who performed preliminary studies on fiber development potential.
- Samrat Mohanty, a graduate student at SIU, for assistance with analytical studies.

Sincerely

Frederick E. Douglas
Principal Investigator

# EXECUTIVE SUMMARY

Integrated Gasification Combined Cycle (IGCC) plants produce a large volume of solid byproducts, just like pulverized coal combustion (PCC) plants. It is estimated that a 425 net MW IGCC plant burning 10% ash coal will produce about 450 to 500 tons per day of solid byproducts. These can be separated into two fractions: a coarse vitreous fraction (FRIT) and a carbonaceous fines fraction (CFF). The CFF fraction, which has a high heating value is generally recycled through the gasifier as a fuel source to improve coal utilization. The FRIT fraction may be used as an abrasive, in cement-concrete applications, or as road sub base material. The physical and chemical properties of such solid byproducts are different from fly ash and bottom ash produced from PCC plants. Therefore, development of gasification byproducts utilization strategies that are economic and environmentally sound is essential for the commercialization of IGCC technology.

The overall goal of this project was to perform an exploratory study for utilizing IGCC solid byproducts to develop value- added novel materials beyond already explored cement- concrete applications. The more specific objectives of the project were to:

1) Characterize different fractions of gasification byproducts from the Power plant from a materials development point of view. These characterization studies were to include thermal, physical and chemical analyses.

2) Based on the data from (1) above, identify at least two (2) novel applications for "medium-volume utilization" for one or more of the gasification byproducts fractions.

3) Perform laboratory studies on a limited scale to develop and characterize the novel materials produced in this study.

The studies completed here indicate that IGCC byproducts vitrified coarse fraction (FRIT) has properties very similar to glass and has potential for development into glass fibers, and associated materials such as rock wool, substrates for solar energy absorption, obscuring material for military applications, and decorative tiles for the external/ internal surfaces of buildings. The FRIT also has potential to be used as an insulating material for steel beams, partly due to its high melting temperature of 1600° C. The idea is to insulate steel beams in high rise buildings with this material. In the event of a fire, the FRIT would increase the time it would take for the steel beams to reach their softening, temperature limit and could conceivably prevent building collapse.

Most operators currently recycle the fines fraction, with much higher heating value, into the gasifier. The ash content of this carbonaceous fraction eventually gets converted to the FRIT fraction during the recycle gasification step.

The authors believe that more in-depth development studies should now be undertaken for development of one or more innovative materials with medium to large volume utilization potential from the FRIT. The innovative materials and applications identified in this study include substrates for solar energy absorption, obscurance material for military

applications, insulating materials and decorative tiles for the building industry. These are new markets with significant potential.

# ABSTRACT

This project has performed an exploratory study for utilizing IGCC solid byproducts to develop value- added novel materials beyond already explored cement- concrete applications, or lightweight aggregate. The results indicate that IGCC byproducts vitreous coarse fraction (FRIT) has properties very similar to glass and has potential for development into glass fibers, insulating materials such as rock wool, substrates for solar energy absorption, obscuring material for military applications, and decorative tiles for the external/ internal surfaces of buildings. Most operators currently recycle the carbonaceous fines fraction (CFF) as a fuel source due to its relatively high heating value. Ash content of this fraction eventually gets converted to FRIT during the recycle gasification step.

The authors have identified a number of novel materials and applications. The next step would be to develop one or more of the above mentioned materials further, after some additional screening of these materials and their applications. Only materials with medium to large volume utilization potential would be developed further.

# 1.0 INTRODUCTION

## *1.1 Background and Problem Statement*

Electricity generation using coal gasification, combined with CO2 capture and storage, is an emerging commercial technology. An Integrated Gasification Combined Cycle (IGCC) plant, with available commercial technology, can provide thermal conversion efficiency to electricity of about 50% while capturing about 90% of CO2. An IGCC plant would provide electricity with only about one quarter (¼) of the CO2 emissions per net kwh as compared to a state-of-the-art natural gas combined cycle (NGCC) plant (Reuther, 2003). Gasification can also be used to produce valuable feedstock from coal such as transportation fuel, hydrogen and synthetic natural gas and other valuable materials.

IGCC plants also produce a large volume of solid byproducts just like pulverized coal combustion (PCC) plants. It is estimated that a 425 net MW IGCC plant burning 10% ash coal will produce about 450 to 500 tons per day of solid byproducts. The physical and chemical properties of such solid byproducts are different from fly ash and bottom ash produced from PCC plants. Therefore, the development of gasification byproducts strategies that are economic and environmentally friendly is essential for commercialization of IGCC technologies.

The U.S. Department of Energy is actively working to assist in the commercialization of IGCC technology. Currently, only two IGCC electricity producing demonstration plants are operational in the USA, TECO Energy in Florida and Wabash River in Indiana.

This project has evaluated the feasibility of using IGCC solid byproducts for developing value-added, medium-volume or large-volume usage novel materials. Specifically, the study developed lab samples of the following products: glass fibers, foamed glass, and microspheres. The study also identified a number of potential uses such as, specialized insulating materials, substrates for solar energy absorption, and obscurance materials for military applications, and decorative tiles.

## *1.2 Goal and Specific Objectives*

The overall goal of this project was to perform an exploratory study for utilizing IGCC solid byproducts for developing value- added novel materials beyond already explored cement- concrete applications. The more specific objectives of the project were:

- Characterize different fractions of gasification byproducts from the Wabash River Basin plant from a materials development point of view. These characterization studies were to include thermal, physical and chemical analyses.

- Identify at least two (2) novel applications for “medium-volume utilization” of one or more fractions of gasification byproducts, based on the data developed above.

- Perform laboratory studies on a limited scale to develop and characterize novel materials for applications identified above.

  Deliverables will include a final report of all the completed work along with laboratory size samples of developed materials.

### *1.3 Overall Project Management*

Mr. Frederick Douglas, President of Cosmos Technologies, served as the Principal Investigator on this project. Dr. Y.P. Chugh, an academician and researcher with a strong background in combustion byproducts management worked with Mr. Douglas in planning and execution of this project. Dr. Carlo G. Pantano, a highly recognized glass specialist, and Mr. Robert Schaut a PhD student, both with the Materials Research Institute (MRI) at the Pennsylvania State University provided laboratory research assistance during the efforts to develop potential novel materials.

The final report was prepared by Mr. Frederick Douglas and Dr. Y. Paul Chugh, with contributions from Dr. Carlo G. Pantano and Mr. Robert Schaut. The entire report was reviewed by the project team and discussed prior to submission as a final report to the National Energy Technology Laboratory (NETL).

### *1.4 Overall Report Layout*

The following is a description of the layout of this report. Section 2 provides a summary of previous research work conducted by other researchers. Section 3 outlines the overall research program and experimental studies. Section 4 presents results of characterization studies for the carbonaceous fines (CFF) and vitreous fraction (FRIT). Section 5 summarizes utilization potential studies and their results. Section 6 provides a summary and recommendations.

# 2.0 PERTINENT LITERATURE REVIEW

## *2.1 Introduction*

Solid byproducts from an IGCC unit consist primarily of granular silicate- rich vitreous material (slag or FRIT), and an un-burnt carbon rich fines fraction (CFF) in the form of char.

## *2.2 Previous Studies on Utilization of IGCC Byproducts*

Praxis Engineers, Inc (2000), with funding from the Electric Power Research Institute, (EPRI), the U.S. Department of Energy (USDOE), and Illinois Clean Coal Institute (ICCI), demonstrated that slag can be used as aggregate in cement – concrete and asphalt, roofing shingles, and abrasive materials. Char can be easily separated from slag using physical separation techniques. The removal of char enhances slag properties for use in construction applications. Praxis also demonstrated that lightweight and ultra lightweight aggregate could be produced from slag to develop construction materials with enhanced sound and insulation properties. They also reported that the energy requirements for producing synthetic lightweight aggregate using slag are significantly lower than using clays or perlite.

Wabash River IGCC demonstration plant reported that coal ash was converted to a low – carbon vitreous slag, which is impervious to leaching and may be used as aggregate in construction or as grit for abrasives and roofing materials. Most of the solid byproducts were marketed beneficially. The production of such materials was however small.

Charah Environmental of Madisonville, Kentucky, in cooperation with the University of Kentucky, demonstrated for the IGCC byproducts from TECO Energy Demonstration Plant in Florida, that the byproducts can be separated into three fractions: vitreous material or frit, carbon rich- char and fines.

Chugh and Patwardhan (2002) demonstrated a physical separation technique to separate slag from char based on size separation and flotation techniques. These studies were performed for TECO IGCC byproducts.

Under DOE Cooperative Agreement DE-FC26-04NT42204, Norton (2004) of Mississippi State University studied incorporation of gasifier slag for enhancement of structural foam glass materials. The author demonstrated that the addition of the slag significantly increases the compressive strength of the foamed glass. Norton, Palmer, and Ramsey (2006) completed a study to enhance structural foam materials through incorporation of gasifier slag (FRIT). The project concluded that 1), the addition of small amounts of FRIT results in significant increase in abrasion resistance and a moderate increase in mechanical strength, 2) the process allows improved abrasive resistance at no additional cost, and 3) improved materials could create an insulation market for the buildings industry. The authors suggest development of stronger materials for protective armor. The foamed nature of glass can provide an energy absorbing barrier for impacting weapons.

The University of Kentucky is currently performing a study to evaluate separation of different fractions from IGCC byproducts for large volume utilization. The DOE contract number for this project is (DE-FC26-04NT42203). More specifically, the investigators are demonstrating separation of about 100-tons of byproducts, from Polk Power Station in Florida and Eastman gasifier in Tennessee, into carbon-rich fraction (CFF) and vitreous fraction (FRIT) using a pilot scale truck mounted facility. The investigators identified potential applications for CFF to include 1) recycle fuel to gasifier, 2) cement kiln fuel, and 3) adsorbent materials. Potential applications for the FRIT fraction include use as an additive in kiln feed, pozzolonic concrete additive, roofing granules, or blasting grit. Both the FRIT and CFF are being characterized in this study for environmental properties. However, at the time of this writing, the final report for the project was not available.

IGCC byproducts utilization studies are limited to date and they have focused on large volume usage.

## 3.0 OVERALL RESEARCH PROGRAM AND EXPERIMENTAL STUDIES

This research was subdivided into two major tasks:

1) Byproduct characterization studies, and
2) Materials development studies.

A brief description of each task and their subtasks is given below.

### *Task 1: Byproduct Characterization Studies:*

The overall goal of this task was to develop physical, chemical, and material science characteristics of the FRIT and CFF byproducts fractions from the Wabash IGCC gasifier. However, since the Wabash gasifier was shut down for an indefinite period during the course of this study, NETL approved conducting these studies using IGCC byproducts fractions from Tampa Electric (TECO) gasifier. The data developed in this portion of the study was used to identify more than two materials that may have potential to be developed and marketed commercially. The preparation of these materials and the identification of beneficial re-use applications were beyond what has been reported in the literature previously. This task involved several subtasks as given below.

1.0 Synthesis of previous research efforts on IGCC byproducts.

1.1 Identification of the physical, chemical, and material science characterization tests for the study, along with test specifications.

1.2 Performance of characterization tests. In addition to the size distribution, hardness, oxides composition, and elemental analysis tests, material science characterization studies involving X-ray diffraction, scanning electron microscopy (SEM), electron scattering for chemical analysis (ESCA), and thermal gravimetric analysis (TGA) were also performed.

1.3 Synthesis of characterization data. The goal of this task was to evaluate all the properties of these materials to develop potential beneficial use applications from a materials development point of view.

1.4 Identify two materials that could be developed from one or more fractions identified in the sample.

1.5 Develop Task 1 progress report and deliver an oral presentation to NETL.

### *Task 2: Materials Development Studies:*

The goal of this task was to prepare laboratory size samples of two or more products prepared from the FRIT and/ or the CFF fractions and characterize these prepared products for desired properties. The tests selection was based on the identified materials and their proposed use. The following subtasks were identified.

2.1 Prepare sample(s) of the identified material(s)

2.2 Characterize the material(s) for appropriate properties

2.3 Develop preliminary data on the economics of the developed materials

2.4 Prepare and submit final report along with samples of the developed materials.

Technical considerations in materials development included market needs, material purity requirements, environmental issues, process development needs, and economics. A novel material, which has a wide number of applications, with wide ranges of byproduct loading, would have a greater likelihood of success as a viable product.

## 4.0 CHARACTERIZATION STUDIES RESULTS

### *4.1 Sample Collection*

This study was supposed to investigate byproducts from Wabash River IGGC plant in Indiana. Since this plant was shut down, permission was sought from the NETL Project Manager to investigate byproducts from the TECO IGCC plant that uses Illinois Basin coal and pet coke for power generation. During the period of sample collection, the ratio of coal to pet coke was about 60%. The professional staff collected samples of the two byproducts, FRIT and carbonaceous fines fraction (CFF) under the direction of Cosmos' project team. About 500 lbs of the two byproduct fractions were collected and shipped in sealed buckets to Southern Illinois University in Carbondale.

### *4.2 Sample Preparation*

FRIT samples from all the buckets were mixed and homogenized, and then put back into the buckets to represent homogenized representative samples. A similar procedure was also adopted for CFF samples. Representative samples were subjected to characterization studies below according to standard accepted procedures.

### *4.3 Particle Size Distribution*

Particle size distribution studies were performed on the FRIT and CFF fractions. Two 4-lb samples of FRIT fraction were dried in an oven at $100^{o}$ C for 24 hours prior to sieve analysis. The carbonaceous fraction was dewatered prior to oven drying a 4-lb sample. ASTM-D 6913 procedure was followed for testing. The results are presented in Figures 4.1 and 4.2.

Figure 4.1: Particle Size Distributions for FRIT Fraction

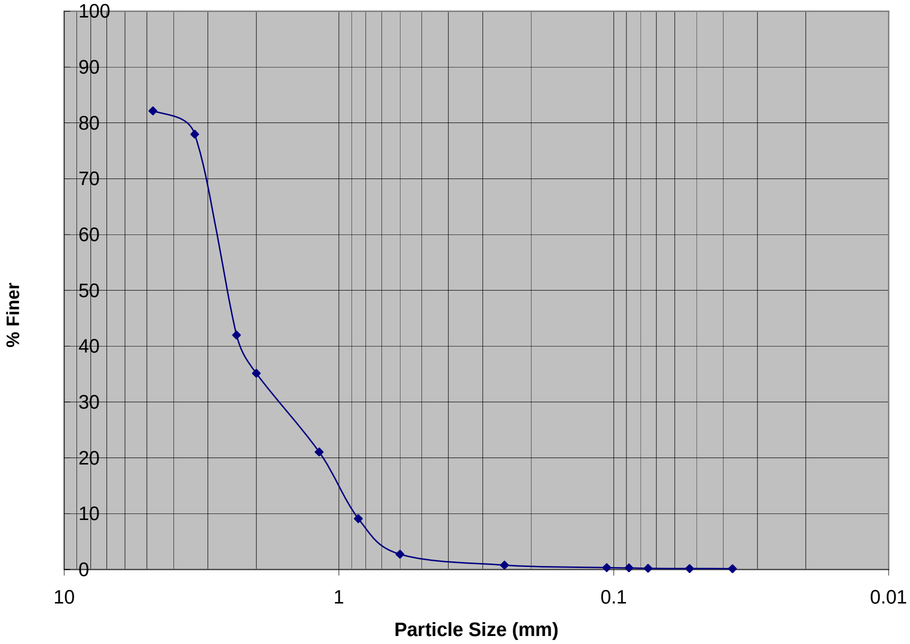

*The mean particle size for the FRIT is about 2.3 mm (Figure 4.1). The uniformity coefficient and coefficient of gradation for FRIT were 3.1 and 1.1, respectively. Therefore, most of the particles are of uniform size.*

Figure 4.2: Particle Size Distribution for CFF Fraction

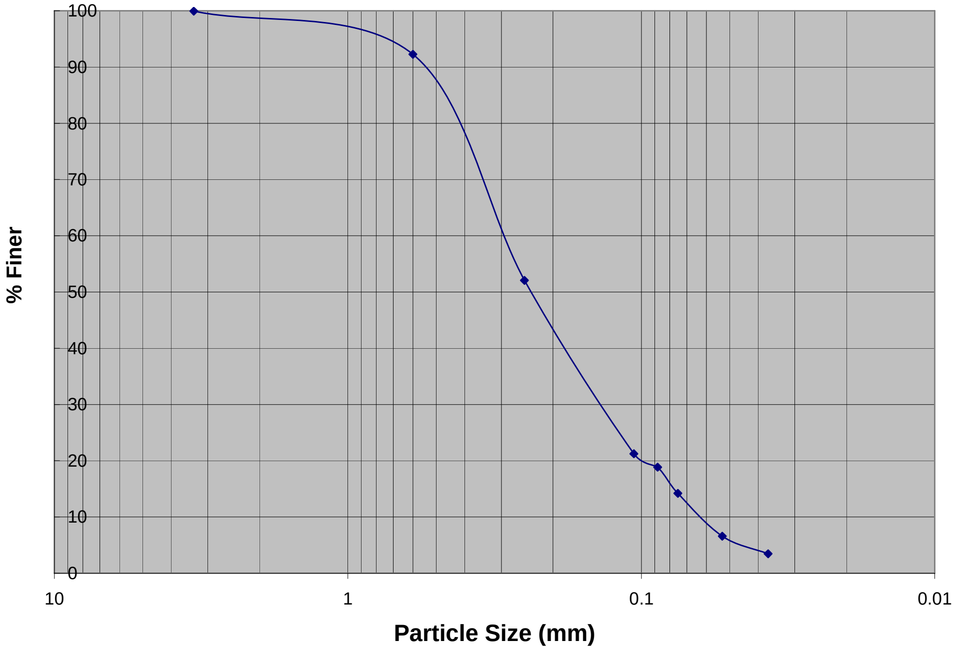

*The mean particle size for the CFF is about 0.23 mm (Figure 4.2). The uniformity coefficient and coefficient of gradation for this fraction were 4.8 and 1.04. Therefore, most of the carbonaceous fraction particles have a wider range of particle sizes than the FRIT fraction.*

## *4.4 <u>Oxides Composition Studies</u>*

Oxides analyses were performed on the FRIT and CFF samples. The results are presented in Table 4.1. The FRIT fraction has substantial amounts of silica, alumina, iron oxides and small percentages of oxides of sodium, potassium, calcium, vanadium and nickel. The CFF has large percentages of silica, iron, sulfur, alumina and small percentages of vanadium, sodium, potassium, calcium, titanium, nickel, phosphorous, and zinc oxides. It also has a small percentage of chlorides. During the period the samples were collected, TECO was processing a mixture of Illinois coal and pet coke. Based on input from TECO professionals, the percentage of pet coke varied but was typically about 25% of the feed. The authors believe that the high nickel concentration is most likely due to pet coke in the feed.

Table 4.1: Oxides composition analyses

| **Carbonaceous Fraction** | | | **FRIT** | |
|---|---|---|---|---|
| **Oxides** | **Weight %** | **Std Error** | **Weight %** | **Std Error** |
| Na2O | 1.45 | 0.06 | 3.06 | 0.09 |
| MgO | 0.43 | 0.021 | 0.989 | 0.049 |
| Al2O3 | 11.27 | 0.16 | 19.87 | 0.2 |
| SiO2 | 26.6 | 0.22 | 54.4 | 0.25 |
| P2O5 | 0.676 | 0.034 | 0.406 | 0.02 |
| Sulphur | 24.18 | 0.21 | | |
| Cl | 1.45 | 0.06 | | |
| K2O | 2.69 | 0.08 | 2.31 | 0.08 |
| CaO | 2.61 | 0.08 | 3.79 | 0.1 |
| TiO2 | 1.15 | 0.05 | 0.962 | 0.048 |
| V2O5 | 6.84 | 0.13 | 2.56 | 0.08 |
| Cr2O3 | < 2*(std error) | 0.033 | 0.095 | 0.012 |
| MnO | 0.0519 | 0.0046 | 0.0523 | 0.0026 |
| Fe2O3 | 16.22 | 0.18 | 10.83 | 0.16 |
| Co3O4 | 0.0149 | 0.0044 | 0.0135 | 0.0014 |
| NiO | 2.69 | 0.08 | 0.415 | 0.021 |
| CuO | 0.233 | 0.012 | 0.0127 | 0.0011 |
| ZnO | 0.577 | 0.029 | 0.0041 | 0.0009 |
| Ga2O3 | 0.121 | 0.006 | 0.0041 | 0.0008 |
| GeO2 | 0.0823 | 0.0041 | | |
| As2O3 | < 2*(std error) | 0.02 | < 2*(std error) | 0.003 |
| SeO2 | 0.0527 | 0.0041 | | |
| Rb2O | 0.0244 | 0.003 | 0.0113 | 0.0007 |
| SrO | 0.101 | 0.005 | 0.0551 | 0.0028 |
| ZrO2 | 0.0621 | 0.0051 | 0.0366 | 0.0018 |
| MoO3 | 0.181 | 0.009 | 0.0235 | 0.0017 |
| PbO | 0.255 | 0.013 | | |

## *4.5 X-ray Diffraction Analyses*

X-ray diffraction tests were performed on both the FRIT and CFF samples. Samples taken from both the fractions were ground to finer than 20 microns. The powder method (ASTM 1365-98) was used to study the structure of the samples. From the test results (Figure 4.3a, b, c), both the materials were amorphous materials with the absence of well defined peaks in the x-ray spectra, which is a characteristic of crystalline solids.

For the obtained x-ray diffraction spectra, a software search and match tool was used to seek the presence of various compounds in both the materials. The spectra of four different iron-silicon oxides are presented in Figure 4.3(a) vis-à-vis the spectra of FRIT and the CFF. As it can be observed, there is no visible perfect match but the presence of two or more of such iron-silicon oxides may lead to the generation of the spectra obtained. Similarly, in Figure 4.3(b) the spectra of both the materials are presented vis-à-vis the spectra of few known silicates of aluminum and vis-à-vis spectrum of graphite in Figure 4.3(c). It may be inferred from the x-ray diffraction analyses that both FRIT and the CFF are composed of unknown compounds of iron, aluminum silicates and carbon.

Figure 4.3 (a)

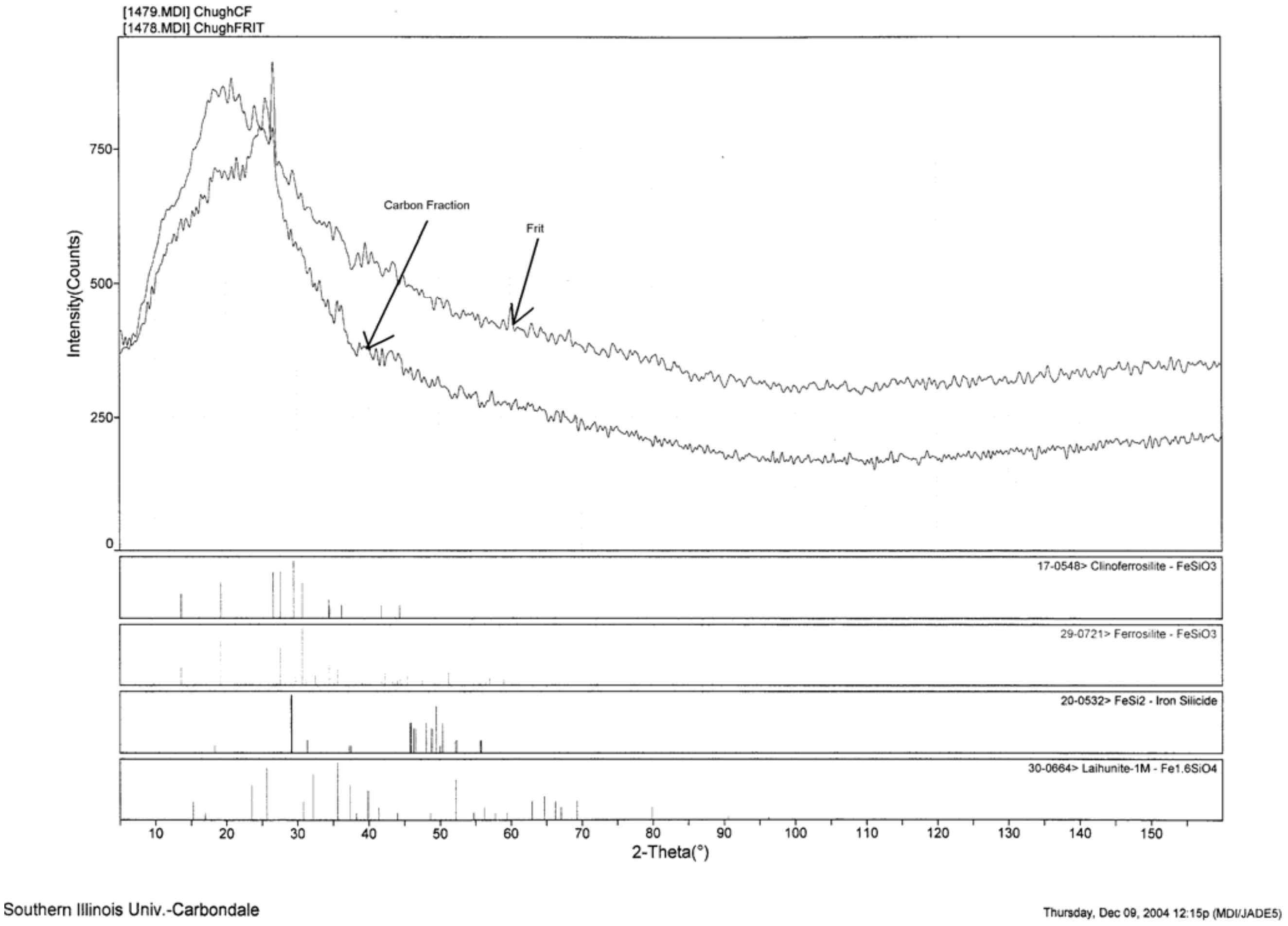
[1479.MDI] ChughCF
[1478.MDI] ChughFRIT
Intensity(Counts)
0
250
500
750
Carbon Fraction
Frit
17-0548> Clinoferrosilite - FeSiO3
29-0721> Ferrosilite - FeSiO3
20-0532> FeSi2 - Iron Silicide
30-0664> Laihunite-1M - Fe1.6SiO4
10
20
30
40
50
60
70
80
90
100
110
120
130
140
150
2-Theta(°)
Southern Illinois Univ.-Carbondale
Thursday, Dec 09, 2004 12:15p (MDI/JADE5)

Figure 4.3 (b)

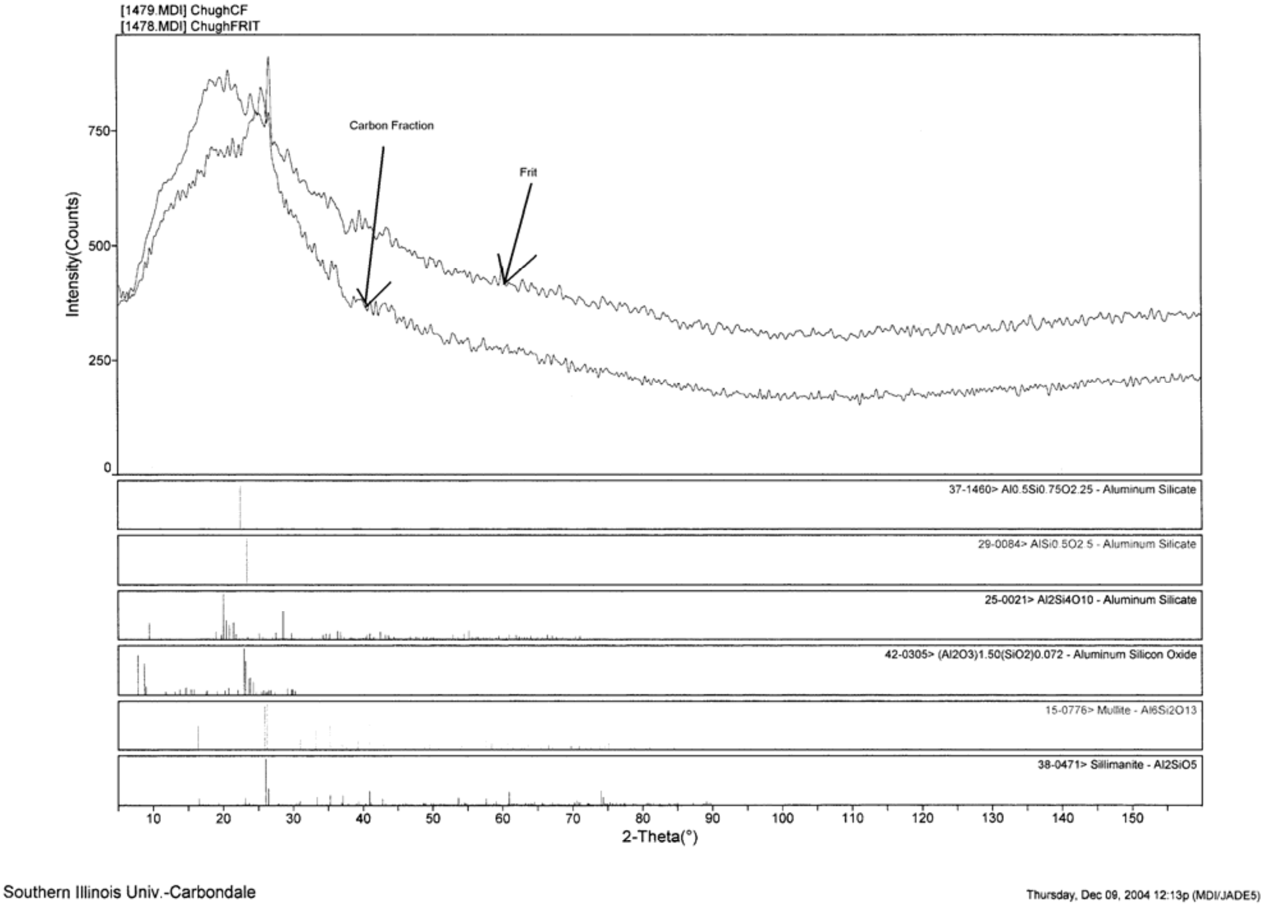
[1479.MDI] ChughCF
[1478.MDI] ChughFRIT
Carbon Fraction
Frit
Intensity(Counts)
750
500
250
0
37-1460> Al0.5Si0.75O2.25 - Aluminum Silicate
29-0084> AlSi0.5O2.5 - Aluminum Silicate
25-0021> Al2Si4O10 - Aluminum Silicate
42-0305> (Al2O3)1.50(SiO2)0.072 - Aluminum Silicon Oxide
15-0776> Mullite - Al6Si2O13
38-0471> Sillimanite - Al2SiO5
10
20
30
40
50
60
70
80
90
100
110
120
130
140
150
2-Theta(°)
Southern Illinois Univ.-Carbondale
Thursday, Dec 09, 2004 12:13p (MDI/JADE5)

Figure 4.3 (c)

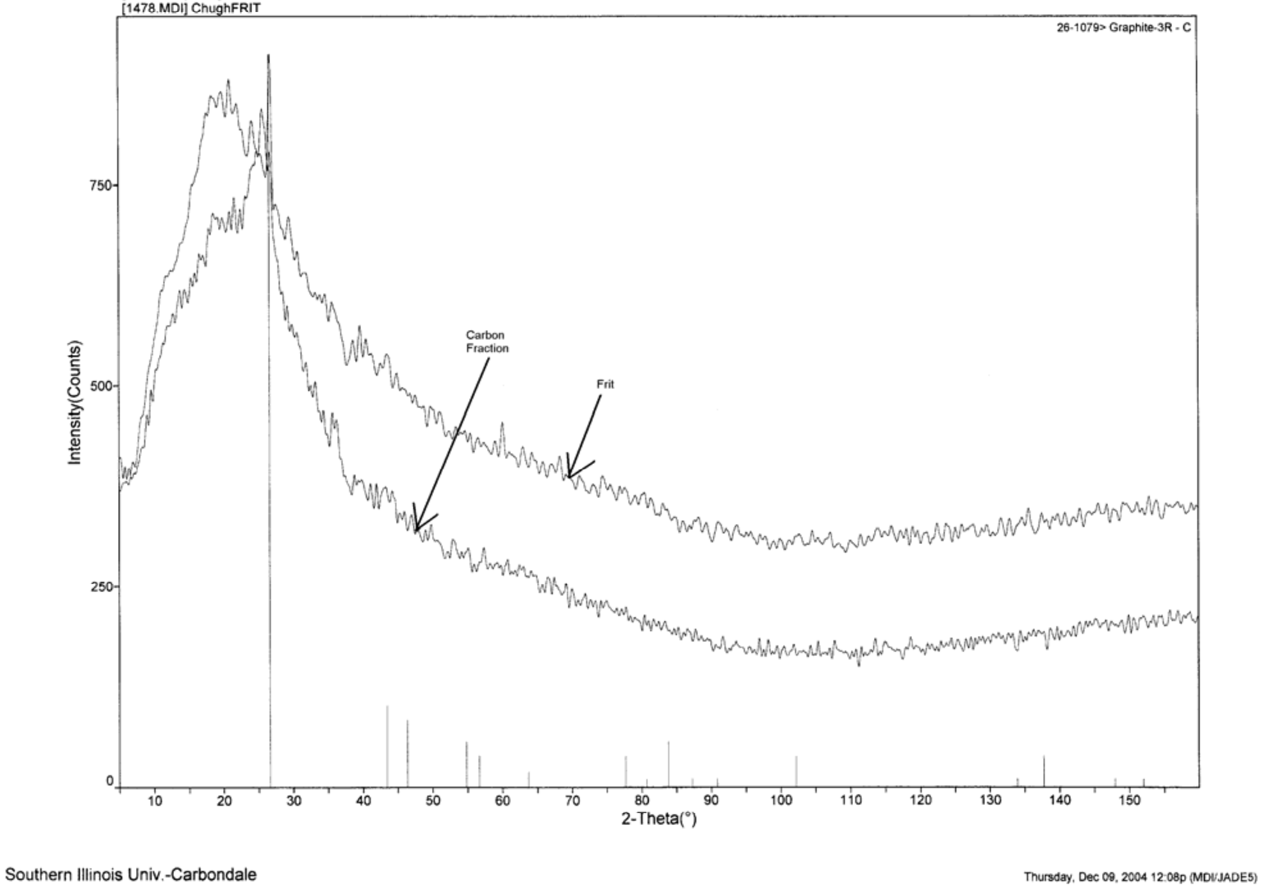
[1479.MDI] ChughCF
[1478.MDI] ChughFRIT
26-1079> Graphite-3R - C
Carbon Fraction
Frit
Intensity(Counts)
750
500
250
0
10
20
30
40
50
60
70
80
90
100
110
120
130
140
150
2-Theta(°)
Southern Illinois Univ.-Carbondale
Thursday, Dec 09, 2004 12:08p (MDI/JADE5)

### *4.6 Scanning Electron Microscope Analyses*

The FRIT and CFF samples were studied under a scanning electron microscope (SEM). Energy dispersive x-ray spectroscopy (EDX) was used to study the elemental spectra of various elements present on the sample surfaces.

A FRIT particle was chosen and its surface was magnified 1000 times to obtain a detailed image of its surface (Figure 4.4). Fine, spherical particles resembling fly ash were observed to be fused to the surface of the FRIT particle. A few random spots of particles were chosen and EDX techniques were used to obtain elemental spectra of those particles. Also, a spectrum was generated from over the entire surface area of the FRIT particle covered in the image.

Figure 4.4: SEM Image of FRIT Particle Surface (1000x Magnification)

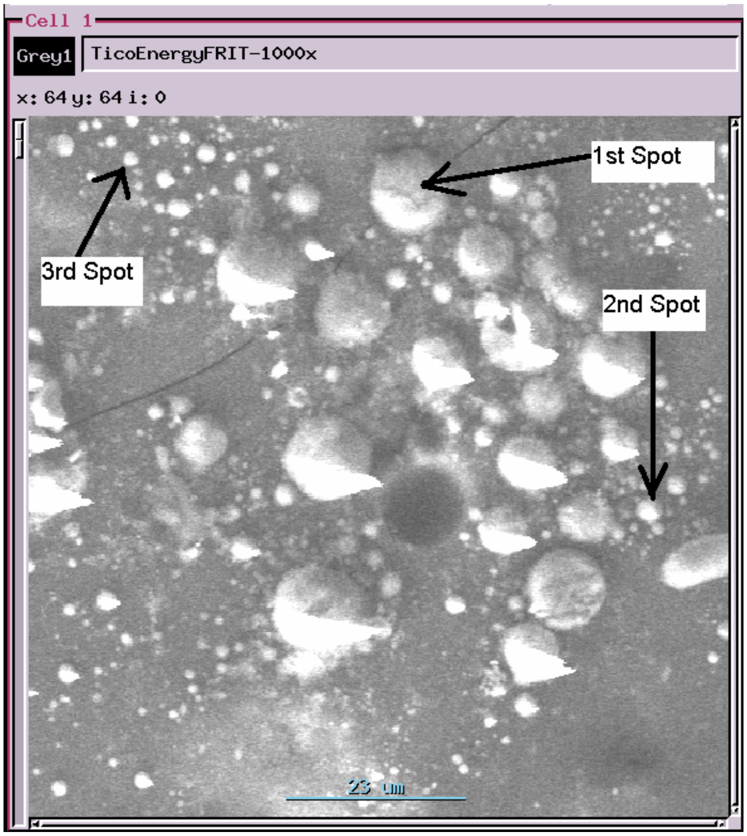

Figure 4.5: EDX Spectrum of the General Area of FRIT Particle Covered In Figure 4.4

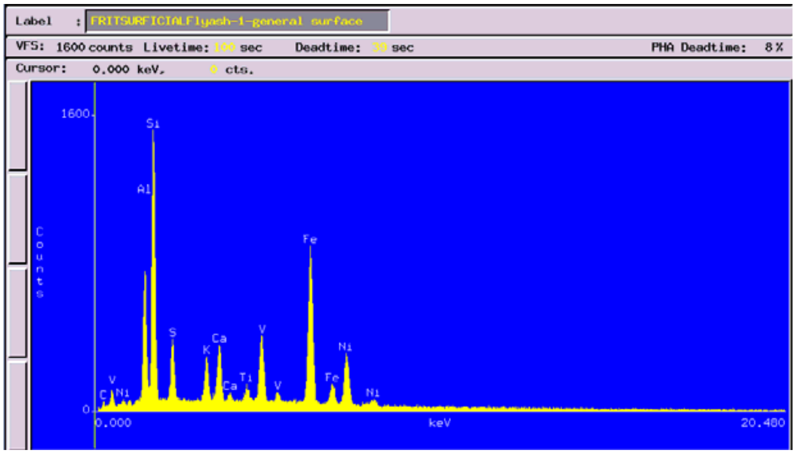

Label : FRITSURFICIALFlyash-1-general surface

VFS: 1600 counts Livetime: 100 sec Deadtime: 39 sec PHA Deadtime: 8 %

Cursor: 0.000 keV. 0 cts.

Figure 4.6: EDX Spectrum Generated From Spot # 1 In Figure 4.4

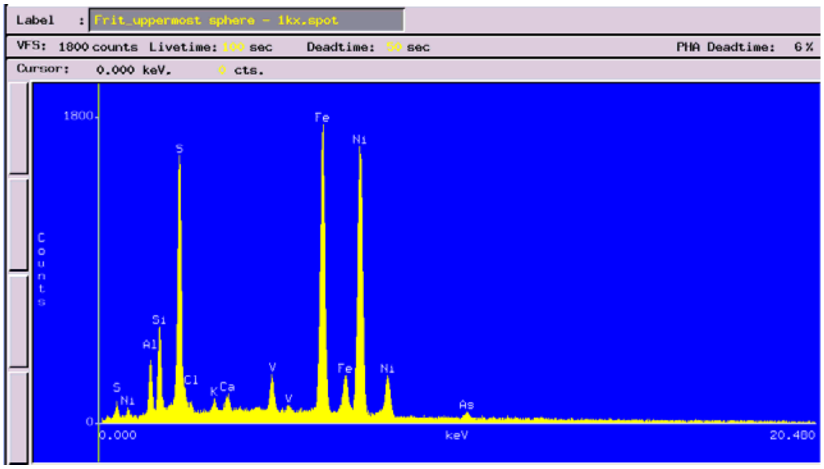

Label : Frit_uppermost sphere - 1kx.spot

VFS: 1800 counts Livetime: 100 sec Deadtime: 50 sec PHA Deadtime: 6 %

Cursor: 0.000 keV. 0 cts.

Figure 4.7: EDX Spectrum Generated From Spot # 2 In Figure 4.4

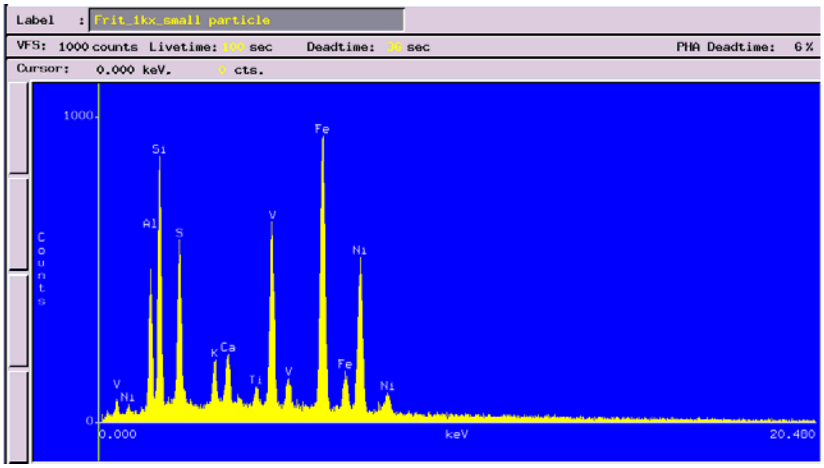

Label : Frit_1kx_small particle

VFS: 1000 counts Livetime: 100 sec Deadtime: 36 sec PHA Deadtime: 6 %

Cursor: 0.000 keV, 0 cts.

Figure 4.8: EDX Spectrum Generated From Spot # 3 In Figure 4.4

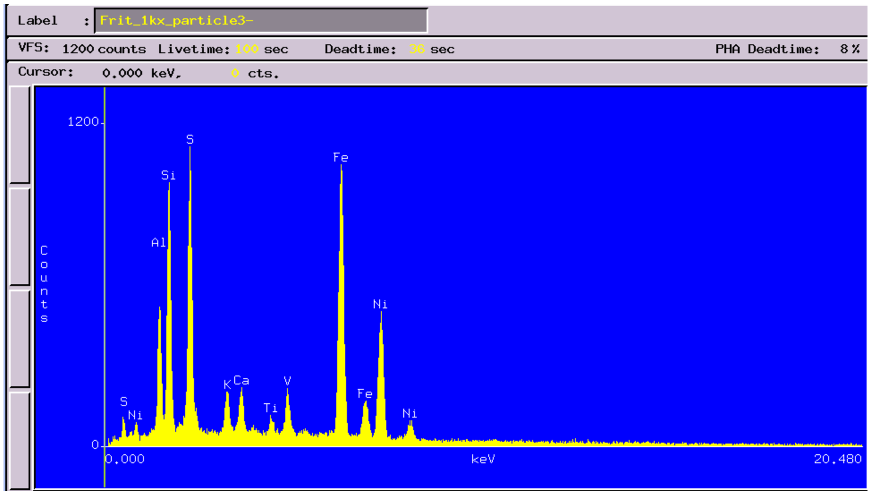

Label : Frit_1kx_particle3-

VFS: 1200 counts Livetime: 100 sec Deadtime: 36 sec PHA Deadtime: 8 %

Cursor: 0.000 keV, 0 cts.

It may be observed from the spectra generated by the particles on the surface of Frit particle that the elemental composition of both the FRIT particle and spherical particles adhering on its surface are overall similar. However, locally there are significant compositional differences. For example, the general FRIT area (Fig. 4.5) has very high Si and Al peaks that are typical of coal fly ash. However, Spot #1 is much higher in S, Fe, and Ni and much lower in Si and Al compared to the FRIT surface. Spot#2 has Si and Al peaks that are similar to the FRIT surface, but its Fe and Ni are higher than the FRIT, and its V peak is much more pronounced than either the FRIT or Spot #1. Spot #3 is generally similar to the FRIT except the S peak for Spot#3 is higher.

Though the spectra obtained presented a qualitative assessment, exact elemental compositions cannot be obtained with a desirable degree of accuracy through the EDX technique.

The CFF was also analyzed under the SEM and the image obtained at 1000x magnification is shown in Figure 4.9. It can be observed from the image that the carbon fraction particles are much finer than the FRIT particles of similar size. Also, few spherical particles can be seen embedded in the fines. Two such particles were chosen for the EDX analyses. EDX spectrum of the entire area covered in the image was also obtained.

Figure 4.9: Image of CFF Matrix (1000x Magnification)

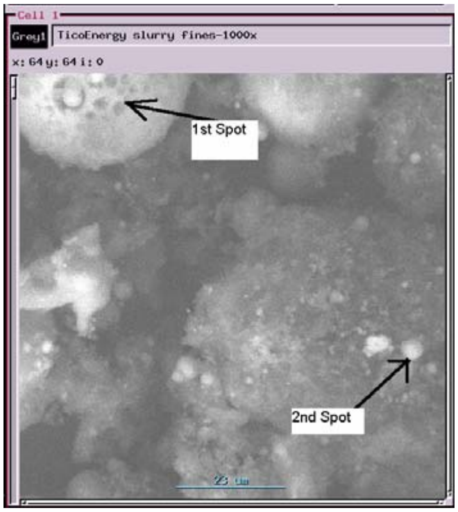

Figure 4.10: EDX Spectrum of General Area in Figure 4.9

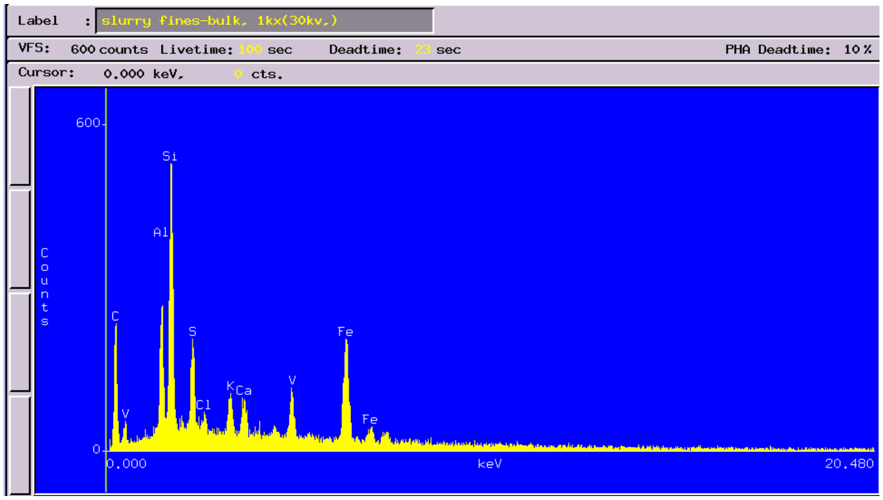

Label : slurry fines-bulk, 1kx(30kv,)

VFS: 600 counts Livetime: 100 sec Deadtime: 23 sec PHA Deadtime: 10 %

Cursor: 0.000 keV, 0 cts.

Figure 4.11: EDX Spectrum Generated from Spot # 1 in Figure 4.9

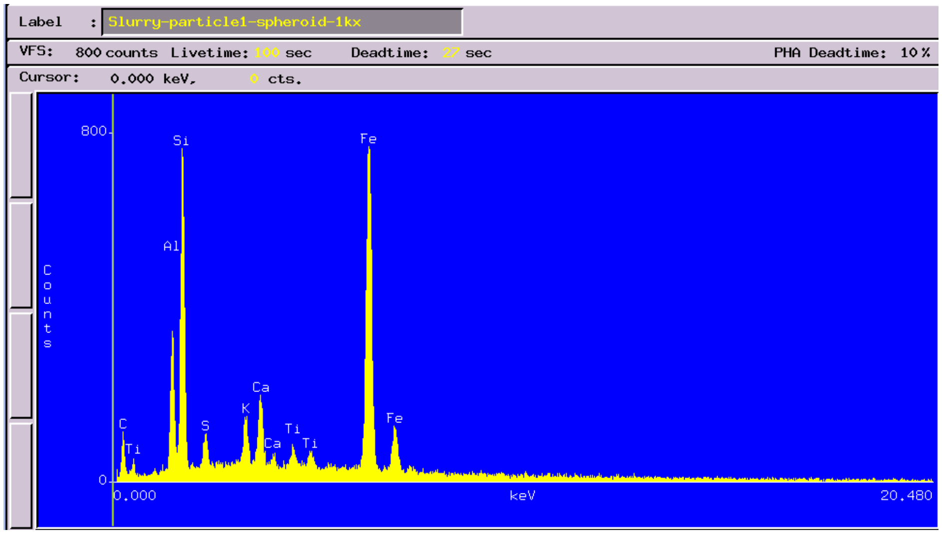

Label : Slurry-particle1-spheroid-1kx

VFS: 800 counts Livetime: 100 sec Deadtime: 27 sec PHA Deadtime: 10 %

Cursor: 0.000 keV, 0 cts.

Figure 4.12: EDX Spectrum Generated from Spot # 2 in Figure 4.9

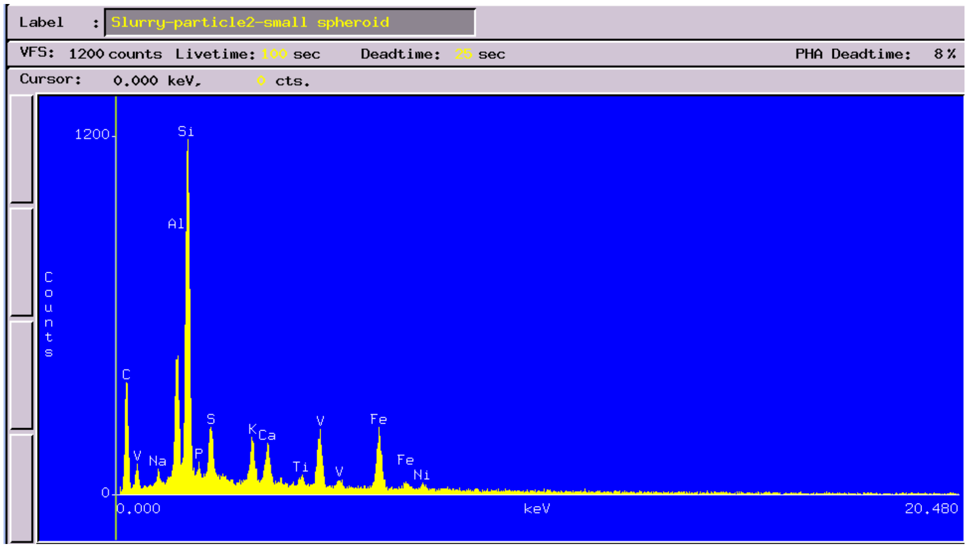

Label : Slurry-particle2-small spheroid

VFS: 1200 counts Livetime: 100 sec Deadtime: 25 sec PHA Deadtime: 8 %

Cursor: 0.000 keV, 0 cts.

It may be observed from the spectra that the general CFF area is similar in composition to that of the FRIT sample, except that a distinct C peak is present in all the CFF spectra and the V and Ni peaks are weak or absent. The EDX spectrum of the first spot in the CFF differs from that of the second spot in that the first spot appears to be richer in iron.

### *4.7 Thermal Gravimetric Analysis/ Differential Scanning Calorimeter Analyses*

TGA/DSC analyses were performed up to 1000° C. The result for the FRIT samples is summarized in Figure 4.13. Very small amount of moisture loss (0.6 %, weight percent) occurs during the temperature range of 600° C to 900° C.

Figure 4:13

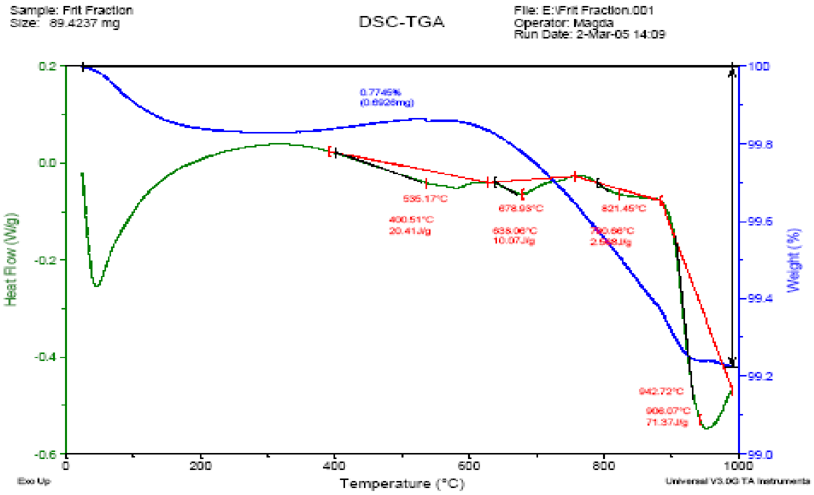

## ***4. 8 ASTM Leachate Test Results***

A variety of methods are used to characterize byproducts and assess their suitability for mine placement or beneficial use. Toxicity Characteristic Leaching procedure (TCLP) is required by most States, but some States use Synthetic Precipitation Leaching procedure (SPLP) or the ASTM Standard Shake Test. The States also differ in the standards they use to evaluate leaching tests and to classify the byproducts. Typically, the leaching test data are compared with either RCRA standards for characteristic hazardous wastes or an end-use water quality standard. Illinois uses Class I groundwater standards as its leaching test limits.

The State of Illinois mandates ASTM standard shake (ASTM D3987-85 (1999)) for evaluating byproducts. This test uses water as the leachant. Seventy grams (70 gms) of the sample is mixed with water (liquid to solid ratio of 20:1) and shaked end-over-end for 18-hours. In addition, leachates were collected from the standard shake test samples at 3, 6 and 9 hour durations to assess time-dependent release of various elements in the leachate. The results are presented in Table 4.2.

Table 4.2: ASTM Shake Test Results

| FRIT | | | | | Illinois Water Quality Standards | |
|---|---|---|---|---|---|---|
| **Samples** | **3-hr** | **6-hr** | **9-hr** | **Standard Shake 18-hour** | **Class I** | **Class II** |
| pH | 4.19 | 4.45 | 4.37 | 4.37 | 6.5 - 8 | 6.5 - 8 |
| Elements (in ppm) | | | | | | |
| Arsenic | 0.02 | 0.02 | 0.04 | 0.02 | 0.05 | 0.2 |
| Boron | 2.45 | 2.7 | 2.77 | 2.96 | 2 | 2 |
| Barium | 0.17 | 0.17 | 0.15 | 0.16 | 2 | 2 |
| Cadmium | 0.22 | 0.23 | 0.25 | 0.24 | 0.005 | 0.05 |
| Cobalt | 0.33 | 0.35 | 0.37 | 0.39 | 1 | 1 |
| Chromium | 0.01 | 0.001 | 0.002 | 0.002 | 0.1 | 1 |
| Copper | 0.48 | 0.34 | 0.38 | 0.32 | 0.65 | 0.65 |
| Iron | 0.74 | 0 | 0.01 | 0 | 5 | 5 |
| Lead | 0.34 | 0.01 | 0.12 | 0 | 0.0075 | 0.1 |
| Manganese | 0 | 0.02 | 0.05 | 0.08 | 0.15 | 10 |
| Nickel | 34.18 | 36.29 | 37.92 | 37.41 | 0.1 | 2 |
| Silver | 0 | 0 | 0 | 0 | 0.0075 | 0.1 |
| Selenium | 0.15 | 0.12 | 0.13 | 0.2 | 0.05 | 0.05 |
| Zinc | 14.41 | 14.4 | 14.4 | 14.4 | 5 | 10 |

Table 4.2: (cont'd) ASTM Shake Test Results

| Carbonaceous Fines Fraction | | | | | Illinois Water Quality Standards | |
|---|---|---|---|---|---|---|
| **Samples** | **3-hr** | **6-hr** | **9-hr** | **Standard Shake 18-hour** | **Class I** | **Class II** |
| pH | 7.5 | 7.28 | 7.28 | 7.04 | 6.5 - 8 | 6.5 - 8 |
| Elements (in ppm) | | | | | | |
| Arsenic | 0.01 | 0.02 | 0.07 | 0.08 | 0.05 | 0.2 |
| Boron | 0 | 0.05 | 0.08 | 0.11 | 2 | 2 |
| Barium | 0.15 | 0.14 | 0.08 | 0.16 | 2 | 2 |
| Cadmium | 0 | 0 | 0 | 0 | 0.005 | 0.05 |
| Cobalt | 0 | 0 | 0 | 0 | 1 | 1 |
| Chromium | 0 | 0 | 0 | 0 | 0.1 | 1 |
| Copper | 0 | 0 | 0 | 0 | 0.65 | 0.65 |
| Iron | 0 | 0 | 0 | 0.01 | 5 | 5 |
| Lead | 0 | 0 | 0 | 0 | 0.0075 | 0.1 |
| Manganese | 0 | 0 | 0 | 0 | 0.15 | 10 |
| Nickel | 0.61 | 1.44 | 2.31 | 1.68 | 0.1 | 2 |
| Silver | 0 | 0 | 0 | 0 | 0.05 | 0.05 |
| Selenium | 0 | 0 | 0 | 0 | 0.05 | 0.05 |
| Zinc | 0 | 0 | 0 | 0.01 | 5 | 10 |

Table 4.2 shows that the FRIT fraction yielded leachates that were acidic. The CFF fraction yielded leachates that were slightly alkaline in the beginning, but at the end of the standard shake test duration, the leachates were neutral. In both the byproducts, the pH and almost all of the trace material concentrations were more or less consistent over a period of 18 hours. Only lead concentration in FRIT decreased from a higher than Illinois Class I and Class II water quality standard values to a value below minimum detection limit.

For leachates generated from FRIT, boron, cadmium, nickel, selenium and zinc exceeded both the Illinois Class I and II water quality standards. The pH was lower than the Class I and II water quality standards. For leachates generated from the CFF, Arsenic and Nickel concentrations exceeded the Class I standards, but were within the Class II standards.

### *4.9 __TCLP Leachate Test Results__*

Since large number of States require TCLP for toxicity characterization of wastes, this test was also performed. This test uses acetic acid or acetate buffer with initial pH of 2.88. One hundred grams (100 gms) of sample is mixed with the liquid- (liquid to solid ratio of 20:1) and leached for a period of 18-hours. Standard TCLP test (US EPA Method 1311) was preformed on both the FRIT and CFF and the results are presented in Table 4.3.

Table 4.3: TCLP Test Results

| **Samples** | **FRIT (-60 mesh)** | **CFF** | **EPA TCLP Hazardous Waste Limit Mg/l (ppm)** | **Illinois Class I (Water quality std)** | **Illinois Class II (Water quality std.)** |
|---|---|---|---|---|---|
| pH | 4.84 | 4.87 | | 6.5 - 8 | 6.5 - 8 |
| **Elements (in ppm)** | | | | | |
| Arsenic | 0.07 | 0.08 | 5.0 | 0.05 | 0.2 |
| Boron | 0.14 | 3.38 | | 2 | 2 |
| Barium | 0.63 | 0.25 | 100 | 2 | 2 |
| Cadmium | 0 | 0.21 | 1.0 | 0.005 | 0.05 |
| Cobalt | 0.11 | 0.34 | | 1 | 1 |
| Chromium | 0 | 0.02 | 5.0 | 0.1 | 1 |
| Copper | 0.25 | 0.28 | | 0.65 | 0.65 |
| Iron | 10.03 | 0.2 | | 5 | 5 |
| Lead | 0.07 | 0.2 | 5.0 | 0.0075 | 0.1 |
| Manganese | 0 | 0.11 | | 0.15 | 10 |
| Nickel | 13.04 | 35.06 | | 0.1 | 2 |
| Silver | 0 | 0 | 5.0 | 0.05 | 0.05 |
| Mercury | Not Tested | Not Tested | 0.2 | 0.002 | 0.01 |
| Selenium | 0 | 0.35 | 20 | 0.05 | 0.05 |
| Zinc | 0.39 | 14.25 | | 5 | 10 |

It is not entirely appropriate to directly compare the results of TCLP tests to Illinois water quality standards. In the strictest sense, TCLP is used to determine whether a material should be considered as "characteristically hazardous" because of the toxicity of its leachate. The results of TCLP are therefore most relevant when compared to the "TCLP Threshold Levels," in Table 4.3 and 4.4.

Both the FRIT and CFF yielded highly acidic leachates at the end of the standard TCLP test. A test for mercury was not conducted. For the characteristic metals tested- arsenic (As), barium, (Ba), cadmium (Cd), chromium (Cr), lead (Pb), selenium (Se) and silver (Ag), the leachate was below the regulated TCLP limits for both the FRIT and CFF fractions. A test for Mercury is required to complete any solid waste classification per this study. In the case of the FRIT, lead, nickel and iron exceeded both the Illinois Class I and II water quality standards. Arsenic exceeded the Class I standard, but not the Class II. In the case of CFF, boron, cadmium, lead, nickel, selenium and zinc exceeded both the Class I and II water quality standards. Arsenic exceeded the Class I standards but not the Class II.

Upon discussion of these results with Mr. Bill Aljoe of NETL, it was decided to repeat TCLP analysis to confirm the results. A comparison of the two sets of data is presented in

Table 4.4. In Table 4.4 the "initial tests" result listed in Table 4.3 were copied into Table 4.4 for quick comparison. The results show that, the leaching increased when the FRIT was sized to a smaller particle size (-60 mesh), compared to the "as received FRIT, which had an average particle size of 2.3 mm. Note that the TCLP characteristic metals tested were all lower than the EPA regulated threshold concentrations. In the case of the initial -60 mesh FRIT sample, nickel and iron exceeded both the Illinois Class I and II water quality standards. Lead and Arsenic exceeded only the Class I standards. In the 2nd -60 mesh sample tested, lead and nickel exceeded both the Class I and II water quality standards. Arsenic, however, did not exceed the Class I or Class II levels. In the case of the "as received FRIT", only Nickel exceeded the Class I and II water quality standards.

The initial TCLP leaching test performed on the CFF fraction, yielded similar results as the second set of tests performed on the CFF fraction. Again, the TCLP characteristic metals tested were all lower than the EPA regulated concentrations in the initial and second set of tests. In both the initial and second set of tests, boron, cadmium, lead, nickel, selenium and zinc exceeded both the Class I and II standards. Beryllium was not tested in the first set of test. In the second set of tests, Beryllium exceeded the Class I, but not the Class II limit. In the initial set of tests, Arsenic exceeded the Class I but not the Class II limit. In the second set of tests Arsenic result was equal to the regulated level of 0.05 ppm.

Table 4.4

| Samples | Initial Test<br>Frit (- 60 mesh) | Frit (as received) | $2^{nd}$ Test<br>Frit (- 60 mesh) | Initial Test<br>Carbon (-60 mesh) Fraction | $2^{nd}$ Test Carbon (-60 mesh) Fraction | TCLP Regulated Levels (mg/l or ppm) | ILLinois Water Quality<br>Class I Std | ILLinois Water Quality<br>Class II Std |
|---|---|---|---|---|---|---|---|---|
| pH | 4.84 | 4.8 | 4.74 | 4.87 | 4.68 | | 6.5 - 8 | 6.5 - 8 |
| **Elements (in ppm)** | | | | | | | | |
| Arsenic | 0.07 | 0.01 | 0.03 | 0.08 | 0.05 | 5.0 | 0.05 | 0.2 |
| Boron | 0.14 | 0.12 | 0.6 | 3.38 | 2.32 | | 2 | 2 |
| Barium | 0.63 | 0.59 | 0.2 | 0.25 | 0.23 | 100 | 2 | 2 |
| Beryllium | | 0 | 0 | | 0.006 | | 0.004 | 0.5 |
| Cadmium | 0 | 0 | 0 | 0.21 | 0.2 | 1.0 | 0.005 | 0.05 |
| Cobalt | 0.11 | 0.08 | 0.49 | 0.34 | 0.3 | | 1 | 1 |
| Chromium | 0 | 0 | 0.02 | 0.02 | 0.05 | 5.0 | 0.1 | 1 |
| Copper | 0.25 | 0.14 | 0.49 | 0.28 | 0.06 | | 0.65 | 0.65 |
| Iron | 10.03 | 3.54 | 1.53 | 0.2 | 0.34 | | 5 | 5 |
| Lead | 0.07 | 0 | 0.25 | 0.2 | 0.3 | 5.0 | 0.0075 | 0.1 |
| Manganese | 0 | 0 | 0.09 | 0.11 | 0.6 | | 0.15 | 10 |
| Nickel | 13.04 | 9.52 | 54.13 | 35.06 | 36.06 | | 0.1 | 2 |
| Silver | 0 | 0 | 0 | 0 | 0 | 5.0 | 0.05 | 0.05 |
| Selenium | 0 | 0 | 0 | 0.35 | 0.14 | 1.0 | 0.05 | 0.05 |
| Zinc | 0.39 | 0.33 | 2.78 | 14.25 | 13.61 | | 5 | 10 |

## 5.0 UTILIZATION POTENTIAL EXPLORATORY STUDIES RESULTS

### 5.1 *Brief Description of the Glass Frit/ Inorganic Pigment Manufacturing*

The project team investigated the use of the FRIT fraction in inorganic pigments. Inorganic pigments containing glass frit are used to color ceramics, glass, concrete, vinyl and plastics. A brief description of this technology is given in the following paragraph.

Glass frit is a component of the final inorganic pigment medium. Glass frit is produced by heating silicon oxide and certain additives, including fluxing agents in a glass furnace. The molten glass flows into a water bath. The large difference in temperature between the molten glass and the water bath causes the molten glass to solidify rapidly and crack into extremely fine particles. This frit is then reduced to desired particle size by grinding or ball milling.

Inorganic pigments are produced by calcining metal oxides in tunnel kilns. The pigment is further sized by grinding and/ or ball milling. The glass frit is then mixed with the inorganic pigment in varying proportions to produce the inorganic pigment medium (inorganic pigment). The pigment is then sold in a powdered form to be used as colorant in ceramics- such as tiles, glass, concrete, vinyl and plastics.

### 5.2 *Evaluation of Pigment Manufacturing Potential*

The FRIT (vitrified fraction of the IGCC slag) was evaluated by professionals at Ferro Corporation to determine its suitability as a frit material in the making of inorganic pigments. The FRIT was wet milled and screen printed unto glass. The material changed color during the wet milling process from black to gray. The material was then fired or baked. After firing the material became dark tan or taupe. The normal temperature firing range for frit manufactured at Ferro Corporation was $1100^{o}$ F to $1300^{o}$ F. In this range the FRIT fraction did not demonstrate the properties that would make it a good frit for inorganic pigment applications. The material did not show any gloss on the surface. More significantly, the material did not stick to the glass surface when screen printed. It was concluded that this material would not make a typical frit for inorganic pigment application.

### 5.3 *Manufacturing Potential for Rock Wool from IGCC FRIT Material*

Laboratory experiments in COSMOS facilities indicated potential to draw fibers from the FRIT material. The project team thought that these fibers may have potential for use in applications such as polymer concrete, polymer composites, carbon-carbon composites and as glass fibers for insulation applications. In discussing these applications with appropriate industries, it was determined that the composition of the FRIT material was very similar to the raw material from which “rock wool” is manufactured. Since the demand for rock wool for insulation is ever increasing, the project team decided to evaluate the potential for using FRIT to manufacture rock wool.

Several manufacturers of rock wool in Indiana and Ohio were contacted. Samples of IGCC FRIT along with its oxides composition were sent to these manufacturers. Additional discussions with these manufacturers led to the possibility of pilot scale testing of this FRIT for rock wool manufacturing. Unfortunately, none of the manufacturers had a small scale set up to evaluate this potential. One company asked that if we could supply them with several tons of IGCC FRIT, they may be able to evaluate the potential. Since monies were not allocated to evaluate such large scale potential, this idea was not pursued further.

The Energy and Environmental Research Center (EERC) of the University of North Dakota was then contacted to determine if they had facilities to evaluate rock wool manufacturing potential on a small scale. They had done some work in this area using fly ash from the combustion of coal. After considerable effort on the part of EERC, it was determined that their facilities will not allow such evaluation at this time.

In addition, fiber glass manufacturers such as Corning were contacted and requested to assist Cosmos in drawing a small sample of fibers from the FRIT material. These companies declined our request on the basis that ingredients within the FRIT such as aluminum and iron and the high melting temperature of the FRIT could conceivably damage their fiber drawing equipment.

Based on these realities, it was decided to approach Dr. Carlo G. Pantano, a highly recognized specialist in glass, at the Materials Research Institute of the Pennsylvania State University to determine if this could be achieved. He was asked to evaluate glass fiber forming potential of IGCC FRIT, as well as some basic glass properties that would be needed to assess the glass forming process and applications of the frit in general. These studies, along with the results, are described in the following sections.

### *5.4 <u>Evaluation of the Glass and Glass-Fiber Forming Behavior of IGCC FRIT</u>*

A set of three evaluation reports were submitted to Cosmos by Robert A Schaut and Carlo G. Pantano. The following sections describe the studies performed and their results.

The first task was an attempt to make glass by melting the raw FRIT (slag) material. The slag was placed in a clay crucible and heated to 1200°C. As the furnace reached 500-600°C, the material began to crackle and eject from the crucible. A fused silica lid was used to contain the material. As the crucible and slag reached 1200°C, it began to melt and foam. The foamed material occupied approximately twice the volume as the original slag.

The glass foam was analyzed for available surface area by the BET nitrogen-gas method. The results showed an available surface area of 0.775m2/g for this sample of foam. This is not considered an especially high surface area (at least for potential application as an adsorbent), but it could be improved through process control and additives, if necessary.

Laboratory studies need to be done first to demonstrate that the slag foam has desirable adsorbent properties, e.g. for Hg or other heavy metals.

It was hypothesized that the foam created by melting the slag was probably due to dissolved gas in the slag, most likely super-saturation with sulfur dioxide. In order to more controllably melt and form a glass or glass fiber, the glass must be pre-conditioned to remove the gas before reaching high temperatures where the fluid melt allows the gas to evolve spontaneously. Thus, the raw slag was placed in a high-alumina crucible, covered, and heated to 1000°C. The material was held for approximately 18 hours at 1000°C to allow the gases to escape. This pre-treated slag was then heated to 1600°C and held for approximately 3 hours. This yielded a viscous melt that could be poured from the crucible and cast onto a cold steel slab, or used to draw fiber (see below). But unfortunately, the 1600°C melt temperature for this IGCC FRIT material is quite high, and this could limit the "working range" for commercial scale casting and/or fiberizing.

To confirm our understanding of the melt behavior after pre-conditioning, the sulfur content was measured using a Leco titration based analysis (based on ASTM C816-85, 2005). The test indicated that there was 0.30 percent sulfur present (on a weight basis) as SO3 in the raw slag FRIT. The same test was performed on the glass quenched after melting the pre-treated slag FRIT, and found to contain <0.02 weight percent SO3 (the detection limit for this technique.). This confirmed that the high temperature evolution of sulfur was responsible for the foaming, and that the slag pre-treatment and subsequent melting reduced the sulfur content by a factor of 10.

For comparison, commercial basalt glass fibers were re-melted in a clay crucible at 1250°C for less than 1 hour. This basalt melt could be poured and cast into a cold steel slab to form a bulk patty at 1250°C, with a viscosity that was comparable to the slag glass at 1600°C.

The next step was to attempt to pull glass fibers from the melted slag glass. A crucible containing the slag glass was heated to 1600°C and held for three (3) hours. Once the glass was melted, a silica rod was touched to the surface and pulled vertically from the melt to form a fiber. These fibers ranged from 100µm to 2mm in diameter and were very non-uniform in thickness and surface finish. The non-uniform diameter and surface roughness along some regions of the fibers were attributed to the variability in temperature within the melt. The non-uniformity in diameter could be better controlled in the future by pulling the fibers while maintaining a constant temperature of the crucible and melt. Figure 5.1 shows a photograph of the raw slag material, the bulk slag glass, and the thick fibers pulled from the slag glass melt.

Figure 5.1: Photograph of the Raw Slag Material, Melted Slag Glass Pieces, and Slag Glass Fibers. A Ruler is provided for Comparison.

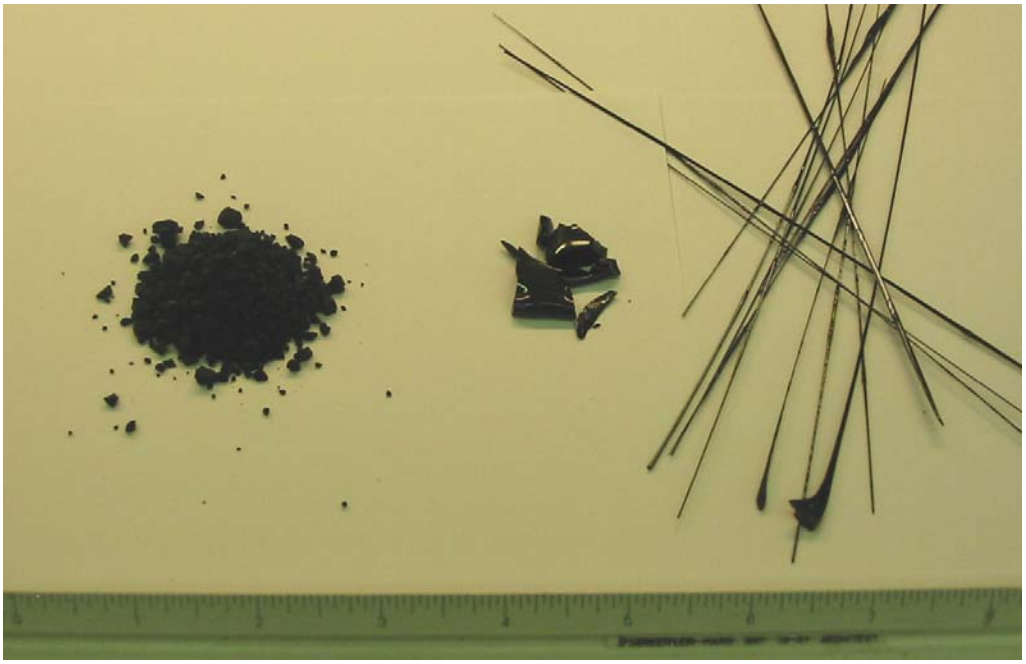

X-ray diffraction is commonly used to check for crystalline phases in glasses. In amorphous samples, the results show a broad ‘hump’ with no defined peaks. Samples with more than 5% crystals will show thin diffraction peaks superimposed upon this ‘hump’. Figure 5.2 shows the XRD results for the remelted basalt glass and the bulk slag glass. The results show that the slag glass contains some crystals, and this confirms the relative instability of the melt. It would be useful to measure the liquid temperature and crystallization rate of the slag glass to better characterize its applicability for glass processing, and to serve as a reference point for the effects of additives to the slag glass that can improve its ability to be processed. The basalt glass fibers result show no signs of crystallinity, but the detection limits for XRD are rather high (~5 vol %). The results for the BULK slag glass show a detectable crystalline peak near 36°. The slag glass fibers were not analyzed.

Figure 5.2**:** X-ray diffraction results for the basalt and slag glasses.

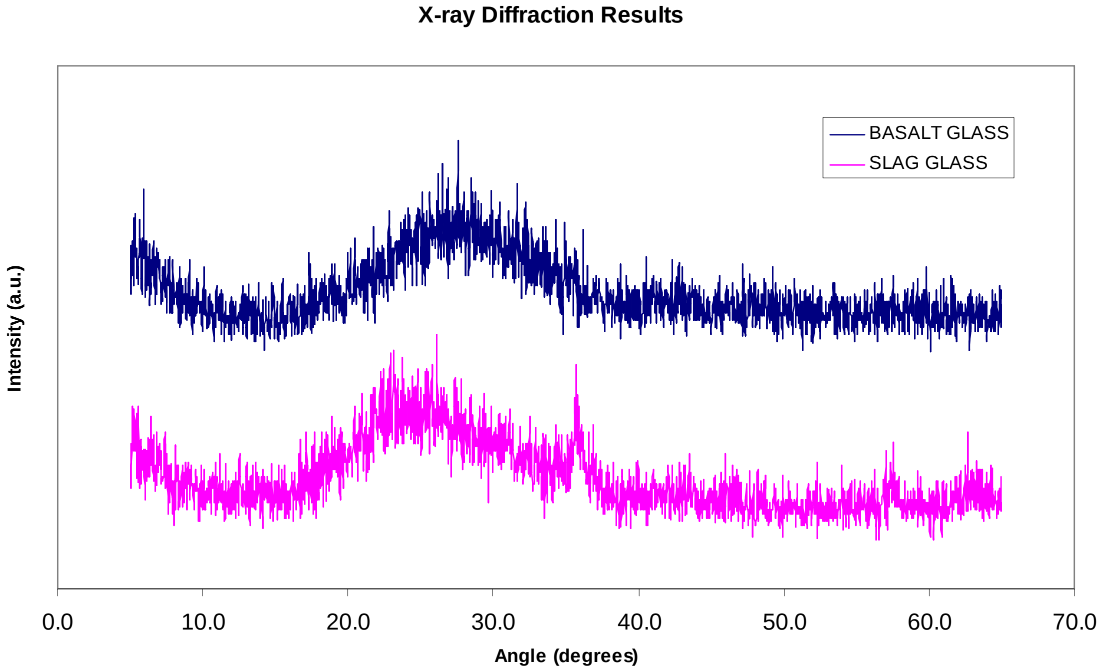

X-ray photoelectron spectroscopy (XPS) is an easy, quantitative method for measuring chemical composition. In this study, samples of the basalt and slag glasses were crushed into fine powders and analyzed. The quantified results are displayed in Table 5.1. The results show that the slag glass has a higher fraction of silica and alumina than the basalt glass. The slag glass also has less alkali and alkaline earth (K, Ca, and Mg) than the basalt glass. Both these differences contribute to the slag glass having a higher melting temperature than the basalt glass. Modifying the slag glass composition with alkali, alkaline earth, or boron oxide would lower the melting temperature and may improve the fiber-drawing behavior of the FRIT glass.

Table 5.1*: XPS Results Showing the Composition of the Basalt and Slag Glasses in Atomic Percent. The Slag Glass is more refractory because it has more Silica and Alumina, and Less Alkali (K, Ca, and Mg) than the Basalt Glass.*

| | Composition in Atomic Percent | | | | | | | | | | |
|---|---|---|---|---|---|---|---|---|---|---|---|
| | Na | Fe | O | K | Ca | C | Mg | Si | Al | Cl | Zr |
| BASALT GLASS | 0.6 | 0.4 | 51.5 | 0.9 | 6.5 | 13.7 | 3.5 | 13.9 | 8.3 | 0.4 | 0.3 |
| SLAG GLASS | 1.1 | 1.0 | 51.1 | 0.6 | 1.4 | 17.2 | 0.4 | 16.7 | 10.3 | | |

Chemical durability, especially to caustic conditions, is important for any application where the glass may be exposed to humid, aqueous, or corrosive environments. Several glasses were tested by immersion in 2N NaOH solution at 70°C for up to 15 hours. This is a common test for glass fiber, and usually reveals how resistant the glass surface is to aqueous weathering and chemical attack by basic (caustic) solutions. The durability is typically reported as a percent weight loss relative to the starting mass. Table 5.2 shows the results of these tests for the raw slag material, slag glass, slag glass fibers, basalt glass, and e-glass. Clearly, conversion of the raw slag into glass has enhanced its caustic resistance. The durability of the slag glass is not as good as other commercial glass compositions, but that could be improved with minor additions to the glass melt. The slag glass fibers showed a higher mass loss than the bulk glass and this is most likely due to the increased surface area available for corrosion. A more meaningful test would compare uniform slag glass fiber with commercial basalt and e-glass fibers (where all fibers have the same surface area). For reference, commercial E-glass and KV basalt fibers exhibit (a reported) 42% and 25% weight loss after 3 hours in 2N NaOH at 100°C (boiling) [Report from Kamenny Vek (Advanced Basalt Fiber Company), www.basfiber.com].

Table 5.2: *Chemical Durability Results for Different Bulk Glass Samples. The Results Show that the Raw Slag Lost 3.4% and the Slag Glass Fibers Lost 1.7% after 15 Hours in 2N NaOh. The Slag Glass Showed 0.7% Weight Loss which was twice that lost by the Basalt and E-Glass Samples.*

| | RAW SLAG | SLAG GLASS | SLAG GLASS FIBERS | BASALT GLASS | E-GLASS |
|---|---|---|---|---|---|
| after 0 hours | 0.0% | 0.0% | 0.0% | 0.0% | 0.0% |
| after 3 hours | 1.2% | 0.3% | 0.1% | 0.1% | 0.0% |
| after 15 hours | 3.4% | 0.7% | 1.7% | 0.3% | 0.3% |

Hardness was also measured for a similar selection of common glasses. A sample of the glass was mounted and polished to a 1μm finish. The hardness was measured using a Vickers-shaped diamond indenter under 200g loads held for 15 seconds before releasing the load. Five (5) indents were made across the polished surface and measurements were made from the tips of the cracks protruding from the indent diagonals. The average hardness values for the glasses are presented in Table 5.3 in both Vicker's hardness units and GPa. The average hardness for the slag glass was higher than all other glasses tested. This is probably due to the presence of micro-crystals in the cast slag glass.

Table 5.3: *Average hardness values for several bulk glasses. The values are an average of at least 5 measurements. The Vickers hardness scale ranges from 100-1000 with increasing hardness.*

| | SLAG GLASS | BASALT GLASS | FUSED SILICA | E-GLASS |
|---|---|---|---|---|
| Ave. Hardness (Vickers Units) | 721 | 678 | 696 | 568 |
| Average Hardness (GPa) | 7.1 | 6.6 | 6.8 | 5.6 |

Summary of Preliminary Glass and Glass-Fiber Making Studies: It is possible to melt and vitrify the IGCC slag material, although it requires higher temperatures than for an E-glass or basalt glass. The resulting slag glass contains some fraction of crystals, at least for the melting conditions and cooling rates used here. It may be possible to lower the melting temperature and reduce the crystalline content by adding a small amount of modifier (such as calcium oxide, lime) to the glass melt.

The molten slag glass is readily drawn into fibers using an up-draw process. The resulting fibers are chemically more durable than the original slag material. The hardness (and probably elastic modulus) of the slag glass is higher than E-glass and basalt, and the durability is reasonable.

Compositional analysis of the slag revealed that it is higher in Si, Al and Fe, and lower in Ca than commercial basalt glass. The susceptibility of the slag to “foaming” during melting is due to excessive dissolved sulfur gas, which can be released at lower temperatures via pre-treatment to in order to vitrify and cast or fiberize the molten slag at higher temperatures. It is possible, however, that the spontaneous foaming of the slag may be an advantage for some applications.

## ***5.5 Studies on Microwave Melting of Slag Glass***

Studies were initiated to assess if microwave melting of glass could be advantageous given the preliminary studies that necessitated very high melting temperatures to process the FRIT as a glass (~1600$^o$ C). The presence of Fe in the glass could facilitate microwave melting, and so preliminary experiments were performed to evaluate this possibility. These studies were pursued with a susceptor and without a susceptor. The susceptor is a shroud that is placed around the crucible to absorb MWs and thereby pre-heat the glass (since most glass does not absorb MWs until reaching temperatures of 300-400$^o$ C). It is demonstrated below that, in fact, the presence of Fe in the FRIT not only eliminates the need for a susceptor, but greatly enhances the microwave processing of the FRIT. Below is a summary of the results.

## ***Microwave Heating Studies With Susceptor***

Studies were done using the following conditions.

| | |
|---|---|
| Sample size: | 115 g |
| Crucible: | 94 g (alumina) |
| Microwaves: | 2.45 GHz, multimode cavity, with turntable, 1 kW then 1.5 kW |
| Atmosphere: | air |

The results showed that it was very easy to heat the slag glass. The temperature profile (Figure 5.3) indicates that the FRIT, itself, is very susceptive to microwaves, and as shown below, does not require pre-heating by the susceptor. The sample got hot immediately and within 3 minutes it reached 400°C. The sample was heated to over 1400°C in several minutes. The temperature profile in Figure 5.3 shows only the top surface temperature of the sample measured with an IR pyrometer (Raytek). Within the 1st 4 minutes, the slope is linear, corresponding to a simple bulk heating. After 4 minutes, the slope changed and the ramping rate was lower, indicating that melting in the center had started. The temperature increased nonlinearly. At 16 minutes, the top surface temperature began to drop, indicating formation of the foamed shell on the top. Due to the increased power input, temperature increased again but very slowly due to the insulating effect of the foam shell. Temperature dropped when the microwave power was shut off at 23 minutes.

Once the microwave heating was stopped, the whole insulated package was taken out of the microwave chamber. The sample was then taken out from the insulated susceptor package and quenched in air. It was found that the top of the sample had overflowed. The overflow was brown foamed glass. After the top was broken and removed, a black solid core was found inside the crucible. The sample was then cut into halves with a diamond saw (Figure 5.4 a-c). Some big cavities were found in the core. Obviously, they were formed at high temperature when the air was trapped in the viscous molten glass.

Figure 5.3: Ramping Profile of the Top Surface of Slag Sample in Microwave Heating (060531).

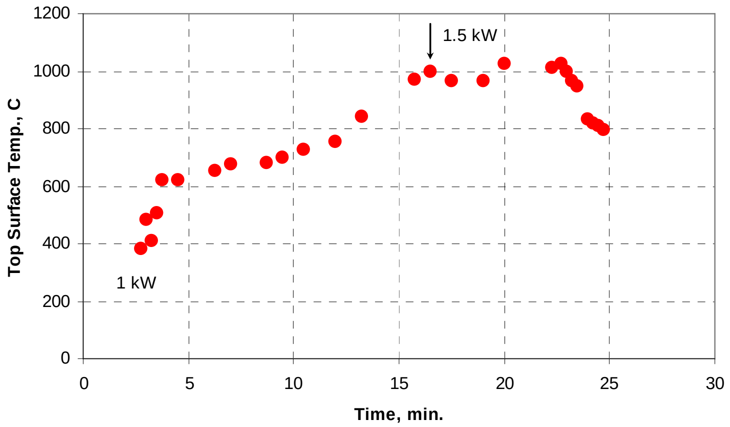

Figure 5.4(a)

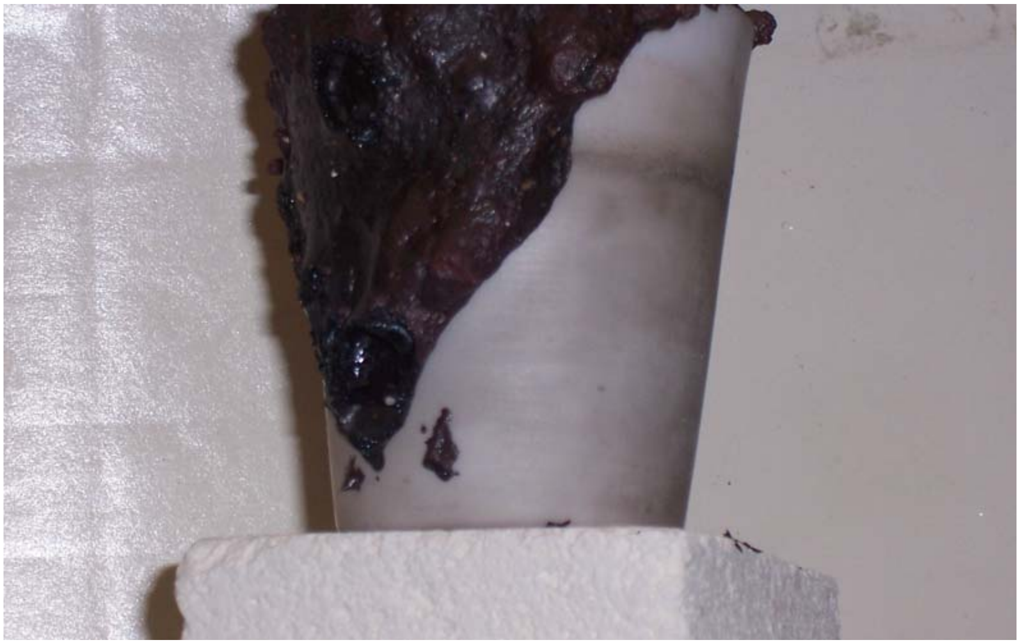

Figure 5.4(b)

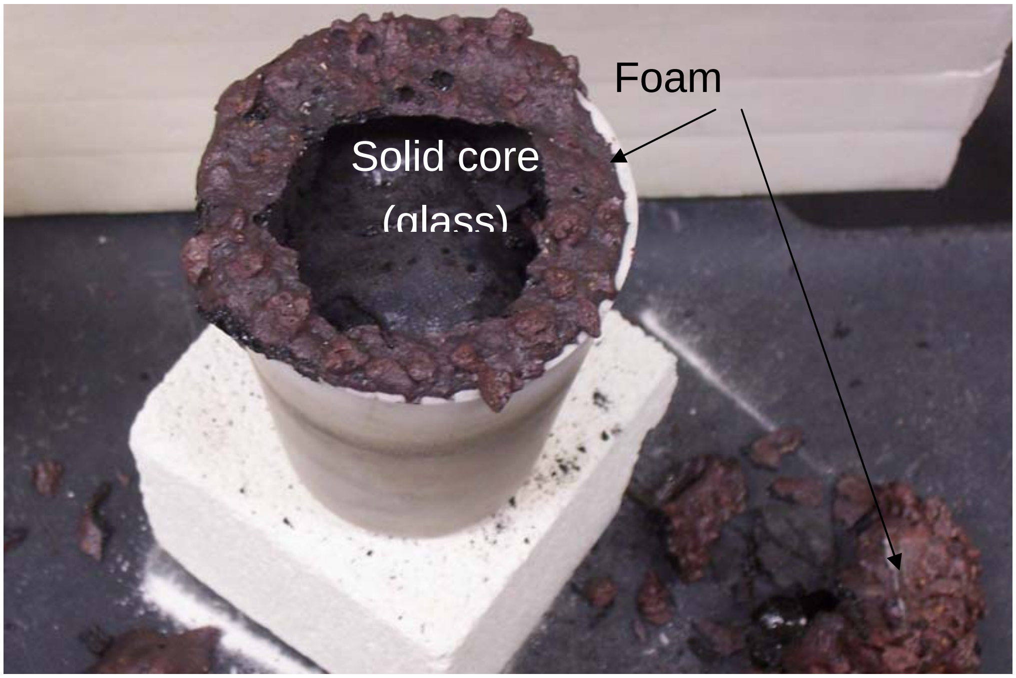

Figure 5.4 (c): The As-Microwave-Melted Slag Glass Samples.

Microwave Melting Studies in Vacuum Without Susceptor

These studies were conducted using the following conditions.

| | |
|---|---|
| Sample size: | 223 g |
| Crucible: | 177 g (alumina) |
| Microwaves: | 2.45 GHz, multimode cavity, with turntable, 1 kW to 2.0 kW. |
| Atmosphere: | Low vacuum (10-20 Torrs) |

This was a larger batch process than before. The crucible was insulated in a FiberMax insulation package with a viewing opening on the top. In order to monitor the temperature of the sample more stably, the viewing opening was made much larger (1.5 in. diameter). However, the large opening increased the heat loss during processing.

During the microwave heating, ionization of the gas in the low vacuum caused arcing in the microwave chamber in the first 10 minutes or so. This phenomenon diminished and finally disappeared after the sample began to absorb microwaves more and more efficiently. The heating profile is shown in Figure 5.5. As previously, this represents only the temperature of the top surface of the sample, which is cooler than the core of the sample, due to the heat dissipation and the foam formation on the top of the sample. The first peak on the profile is believed to be due to the melting of the glass that absorbed more microwave energy. The 2nd peak was due to formation of foam that partially insulated the surface of the sample. Temperature increased due to higher power input. The 3rd peak formed since the power was cut off and sample began to cool.

Figure 5.5: *Temperature profile of the top surface of the slag glass sample in microwave melting without susceptor. Note the peaks distributed in the profile periodically.*

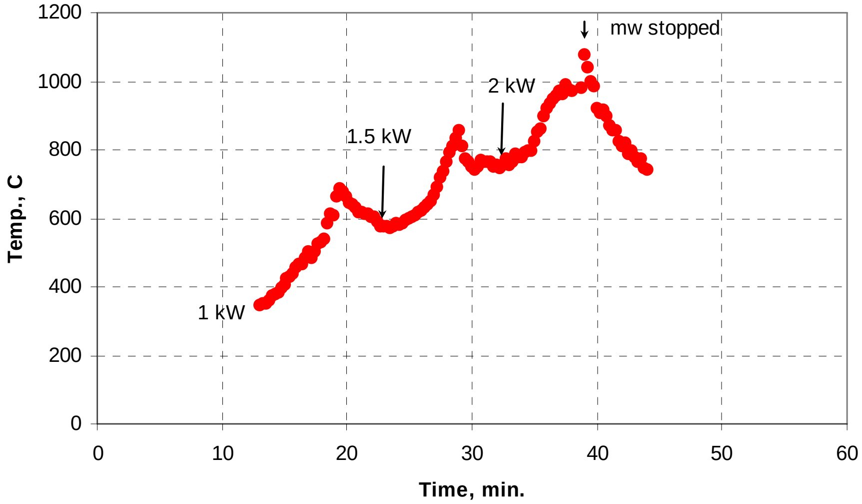

Figure 5.6: *Cross-section of the slag glass melted in microwave low vacuum condition without using any susceptor. The "shiny" specs embedded in the glass are metallic particles (believed to be MAGNETIC iron)*

The results showed that the sample melted in vacuum condition is denser. The large air voids were found on the top of the molten glass. There are fewer voids in the dense glass on the bottom than when it is processed in air.

Summary of Microwave Melting Studies: The IGCC FRIT glass absorbs microwaves efficiently and the samples were melted by microwave heating within minutes. Since the sample is very susceptive to microwaves, it could be easily heated up and melted in microwave vessel even without any susceptor. The structure of the sample melted in vacuum condition was denser than that melted in air. This processing yielded the highest quality bulk glass samples from the slag FRIT, although they contained metallic particles. It is believed that the vacuum melting conditions reduced the Fe-oxides to iron. This can be enhanced or eliminated in the future through controlled atmosphere processing. If magnetic, the particles could provide advantages for EM shielding “coatings” made with the frit, or for magnetic control of the glass spheres (see below).

Analyses of Gases Emitted During the Melting Process: It was thought that an analysis of gases emitted during the melting process was important from environmental point of view. More specifically, concerns were related to remission of captured mercury. Therefore, FTIR studies were performed on the emitted gases. Equipment limitations allowed such studies to be performed only up to 1000$^{o}$ C. The following significant results were recorded.

- An unknown heavy metal organic compound gas was released around 150$^{o}$ C in small amounts and it continued until 600$^{o}$ C.
- CO2 was released throughout the test.
- CO release started around 600$^{o}$ C and increased steadily until the end of the test.
- Sulfur compound gases release started around 400$^{o}$ C and continued until 600$^{o}$ C.
- Small amounts of water was released at 100$^{o}$ C and continued till the end of the test. However, the amount released decreased as temperature increased.

### ***5.6 Feasibility of Developing Flake and Microspheres Using IGCC FRIT***

The foaming nature and high fraction of metals contained within the IGCC slag material could be exploited to create foam or micro-spheres. Either of these could yield (through mechanical crushing) thin, curved “shells” which may act as an airborne obscurant of electromagnetic radiation and/or heat. The micro-spheres, themselves, could also prove useful as low-density-filler for paints, plastics and powder coatings, for civil infrastructure, or for high temperature fluidized bed media.

The first objective of this short-term task was to enhance the degree of foaming to yield large cells with thin cell walls. These experiments were followed with mechanical crushing of the foam to yield "orechietti" (i.e., 'ear'-shaped shells) that would constitute the particulate obscurant or a substrate for such (or possibly a filler material for other applications).

The second objective is to create a complimentary convex surface from the same material by flame spherodization process. In this process, the crushed IGCC slag material is injected into an oxy-propane flame where it melts and forms small spheres. The sphere cools and solidifies as it exits the flame forming glass micro-spheres of various diameters.

The foaming of raw slag material already observed is due to the release of dissolved sulfur as the material is heated. However, better process control is needed to obtain foam with large cells and thin cell walls. A quick literature survey uncovered several patents and technical articles describing the science behind different foaming techniques and methods for creating foamed glass products. Spiridonov et al. (2003) discussed the science behind two common additive-based methods for foaming glass. The first method involves adding salts (typically carbonates) that decompose at various elevated temperatures, where the decompositions products (CO2, H2O, SO3, etc.) create bubbles within the viscous melt. The size of the pores is controlled by the amount of gas released by the decomposing salts. These salt additives are sometimes referred to as neutralization agents. The second method uses 'Redox' gas forming agents which oxidize at elevated temperatures, releasing dissolved gases from within the surrounding glass. These redox agents are typically carbon-based (coke, graphite, silicon carbide). The primary difference between the two types of agents is the resultant pore structure; neutralization agents form maze-like connected porosity whereas redox agents form individual, isolated pores.

Norton, Palmer and Ramsey (2005) studied incorporation of slag or FRIT from IGCC plants into foamed glass to enhance its properties under a grant from the NETL (DE-FC26-04NT422204). The study demonstrated that abrasion resistance of the foamed glass increased significantly and strength increased moderately by adding small amount of FRIT. The study concluded that slag-reinforced foamed glass was superior to base foamed material being marketed.

Initially, to better understand the foaming process, we set out to duplicate the procedures outlined in the patent literature. Using a mixture of crushed soda lime silica glass and various foaming agents, a combination of temperature and foaming agents was found that generated an appropriate pore structure.

The slag material was evaluated in a similar fashion using a variety of foaming agents at different concentrations and temperatures. Eventually, a combination of silicon carbide (SiC) and raw slag material was found to yield the correct pore structure. For that experiment, a batch consisting of 90wt% slag (<180μm) and 10wt% SiC (600 mesh, 16μm) was heated to 1200°C and held for a total of 45 minutes. The resulting foam looked as though it could have foamed to a larger volume, but looked as though the pores were in the correct size range with an optical microscope. Environmental scanning electron microscope (FEI Quanta 200 ESEM) images of grains from this batch are presented in Figure 5.7. In particular, the images show porosity throughout the material over a wide range of sizes, with wall thicknesses near 10µm. Figure 5.8 shows that after lightly crushing the foam in a mortar and pestle (to reduce the foam to ‘orechietti’), the curvature seen in the bulk foam is retained.

Figure 5.7: *ESEM images from the slag glass batch [90wt% slag (<180µm), 10wt% SiC (600mesh)] foamed at 1200°C for 45 minutes. The images show: (upper left) the wide variety of pore sizes ranging from 10 to 1000µm, (upper right) the density of pores and their interconnectivity, and (bottom) pore walls that are less than 10µm thick.*

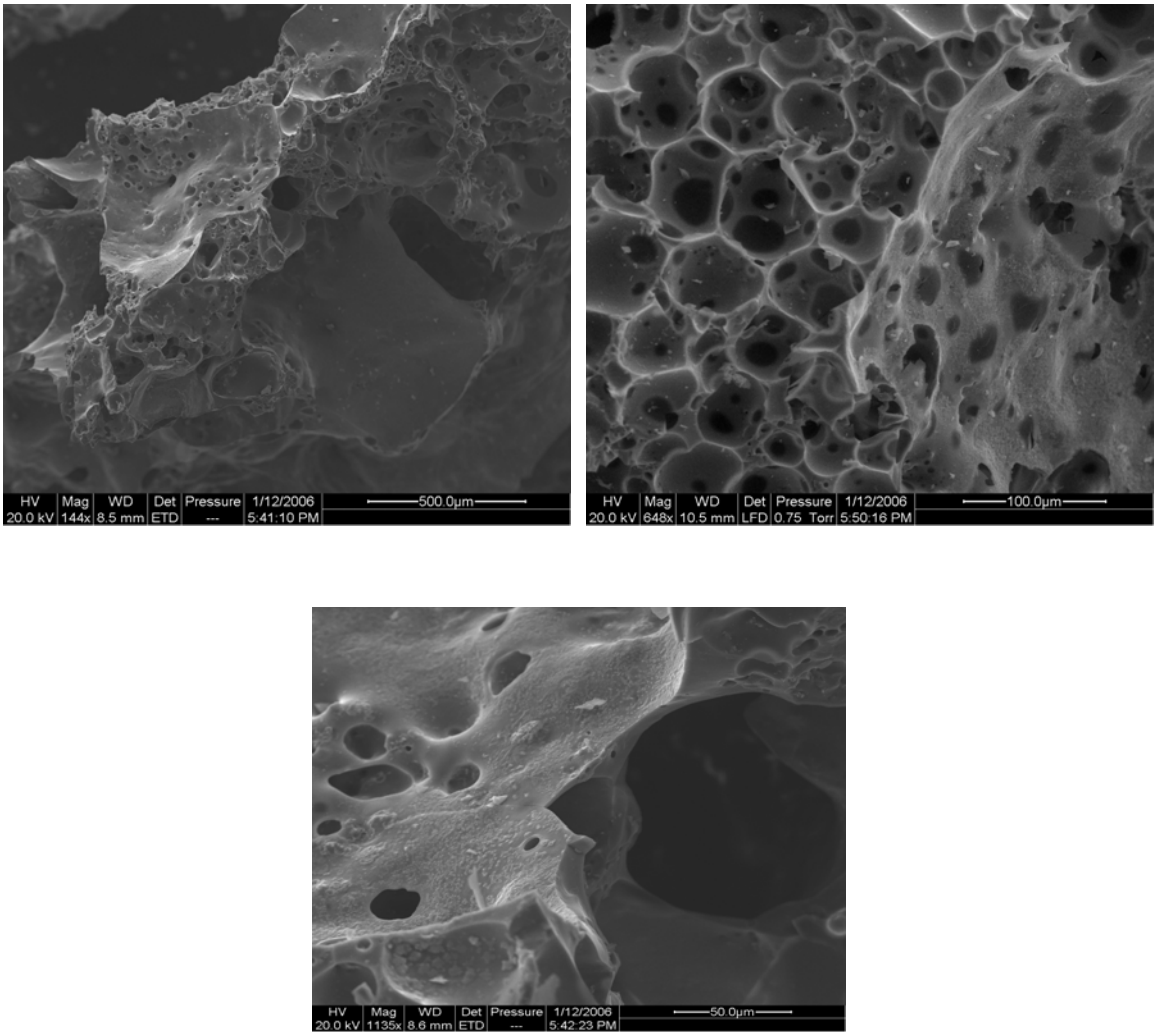

Figure 5.8: *ESEM images of crushed, foamed slag glass [90wt% slag glass (<38μm) and 10wt% SiC (600mesh)]. While curvature is still present, it is not as obvious as in the images of the bulk foam.*

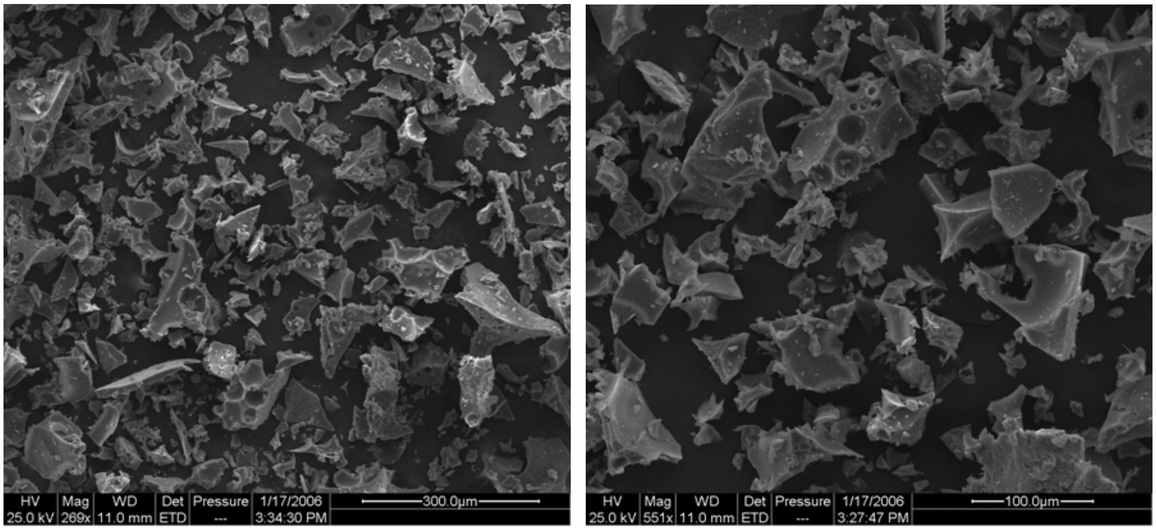

While the surfaces created by foaming the slag material were curved and appropriate for obscuration, it was thought that a more uniform controlled curvature might be possible with glass micro-spheres. Conzone, et al., discuss a method for making solid glass micro-spheres by dropping glass frit into a propane flame. As the particles pass through the flame, they melt and become spherodized before cooling as they exit the flame. A collection tube was set up to gather the spheres as they fell out of the flame. Figure 5.9 shows a schematic of the micro sphere apparatus described by Conzone et al used within this study.

The setup was tested by dropping soda-lime-silicate glass frit (75-150μm) by hand into the propane-air flame. Figure 5.10 shows images of the resulting SLS glass spheres. The non-spherical particles are portions of frit that did not remain in the flame long enough to spheroids. It is likely that this is due to agglomeration of the fine frit which would fall out of the flame well before the glass has had time to spherodize.

The same test was repeated with slag frit that had been crushed to pass a 400 mesh sieve (<38μm). Figure 5.11 shows ESEM images of the resulting spheres. These spheres are quite large and the observed porosity is most likely due to the agglomeration of the fine particles. A different method was devised for dispersing the crushed slag frit before spherodizing. This enabled us to capture particles as small as 2um in diameter. Figure 5.12 shows ESEM images of these smallest IGCC spheres. With more time and an understanding of the process, it would be possible to better control the size of the resulting spheres.

Figure 5.9: *Schematic of the apparatus designed by Conzone et al (2002) for preparing glass micro-spheres.*

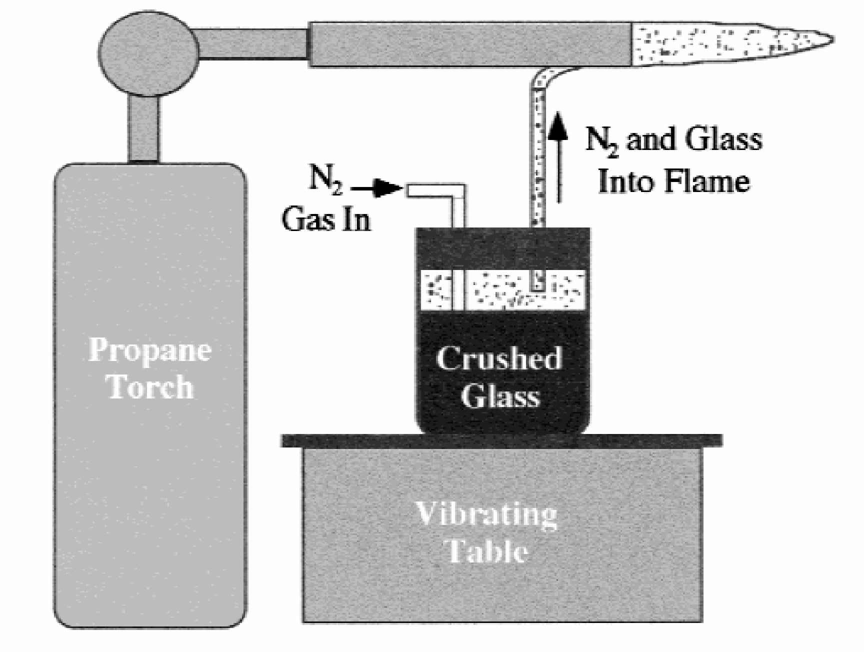

Figure 5.10: *ESEM image of soda-lime-silicate glass micro-spheres created in an air-propane flame. The image shows that while a portion of the particles spherodized, a significant portion did not. The non-spherical particles are probably a result of agglomeration within the starting glass frit.*

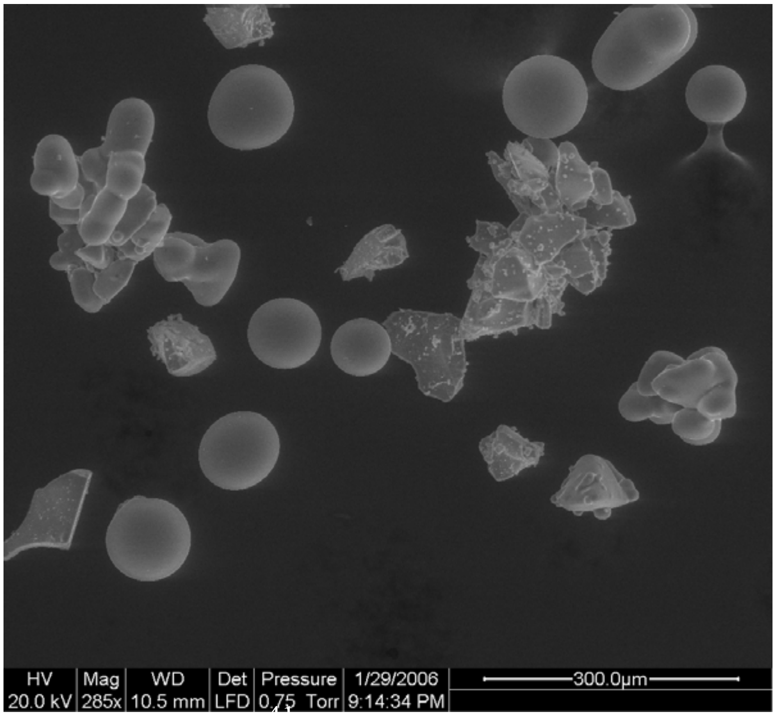

Figure 5.11: *ESEM images of slag spheres created in an oxy-propane flame. The starting frit passed a 400 mesh (<38μm) sieve. The resultant particles range between 50 and 300μm in diameter, showing that the frit must be agglomerating as it is dropped into the flame.*

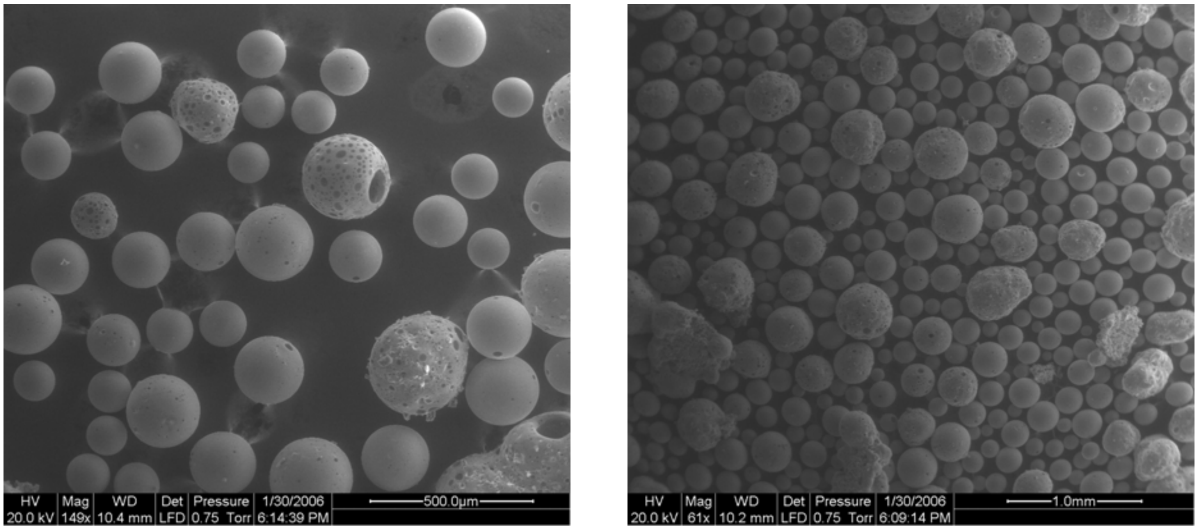

Figure 5.12: SEM images of the smallest slag spheres created by this process.

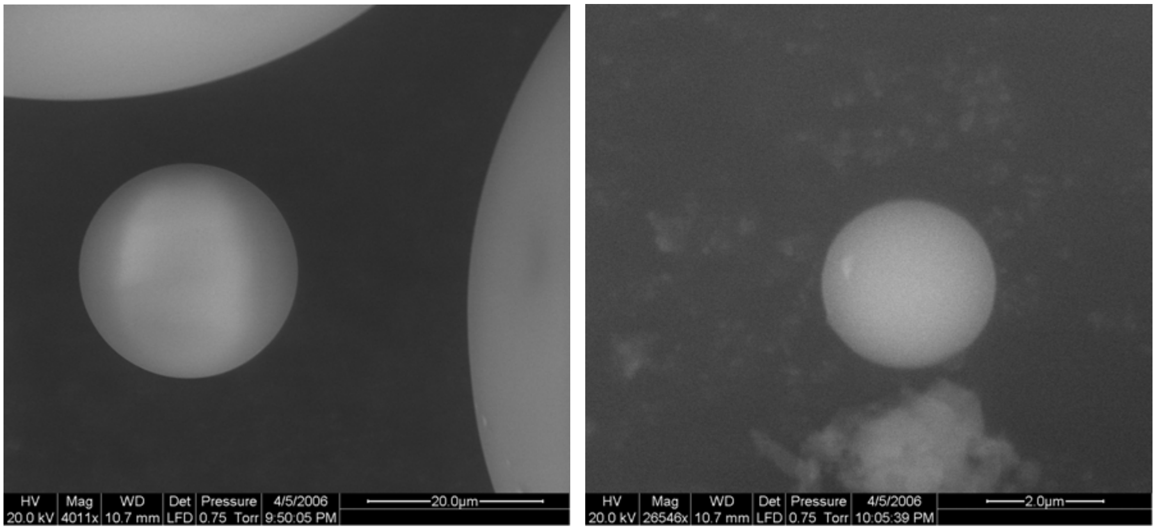

## 6.0 SUMMARY AND RECOMMENDATIONS

### *6.1 Summary*

- The mean particle size for the FRIT is about 2.3 mm. The uniformity coefficient and coefficient of gradation for FRIT are 3.1 and 1.1, indicating that most of the particles are of uniform size.

- The mean particle size for the CFF is about 0.23 mm and the uniformity coefficient and coefficient of gradation are 4.8 and 1.04. Therefore, most of the carbonaceous fraction particles have a wider range of particle sizes than the FRIT fraction.

- The FRIT fraction has substantial amounts of silica, alumina, iron oxides and small percentages of oxides of sodium, potassium, calcium, vanadium and nickel. The CFF has large percentages of silica, sulfur, alumina and small percentages of vanadium, sodium, potassium, calcium, titanium, nickel, phosphorous, and zinc oxides. It also has small percentage of chlorides.

- X-ray diffraction analyses indicate that both FRIT and the CFF are composed of unknown compounds of iron, aluminum silicates and carbon. The presence of two or more of such iron-silicon oxides may lead to the generation of the spectra obtained.

- SEM-EDX analyses for FRIT indicate that the elemental composition of both the FRIT particle and spherical particles adhering on its surface consist of elements like aluminum, silicon, iron, sulfur, iron, nickel, vanadium and titanium in different quantities.

- Locally there are significant compositional differences. For example, the general FRIT area has very high Si and Al peaks that are typical of coal fly ash. However, some spots are much higher in S, Fe, and Ni. Some areas have Si and Al peaks that are similar to the FRIT surface, but their Fe and Ni contents are higher than the FRIT, and their V peak is much more pronounced than the FRIT.

- CFF analyzed under the SEM shows that the carbon fraction particles are much finer than the FRIT particles. Also, few spherical particles are seen embedded in the fines.

- The general CFF area is similar in composition to that of the FRIT sample, except that a distinct C peak is present in all the CFF spectra and the V and Ni peaks are weak or absent.

- The FRIT sample leached boron, cadmium, nickel, selenium and zinc above the State of Illinois Class I and II regulated limits when subjected to the state mandated leach test ASTM shake test (ASTM D3987-85 (1999)), required for evaluating beneficial re-use applications. For the CFF fraction nickel leached above the Class I and II regulated limits and arsenic leached above the Class I limit.

- The FRIT fraction, per the ASTM shake test, yields leachates that are acidic and the CFF fraction yields leachates that are basic.

- When subjected to the TCLP leach test, the FRIT and CFF did not leach any characteristic metal at or above the regulated threshold levels. The metals tested in this study were arsenic, barium, cadmium, chromium, lead, silver and selenium. Mercury was not tested. A test for Mercury is required to complete any solid waste classification per this study.

- Ferro Corporation concluded that this material would not make a typical frit for inorganic pigment application.

- The composition of FRIT material is very similar to the raw material from which "rock wool" is manufactured. However, pilot scale equipment was not available to evaluate rock wool manufacturing potential.

- FRIT can be melted, although it requires higher temperatures than for an E-glass or basalt glass. The resulting glass contains some fraction of crystals, at least for the melting conditions and cooling rates used in this study.

- It may be possible to lower the melting temperature and reduce the crystalline content by adding a small amount of modifier (such as calcium oxide, lime) to the glass melt.

- The molten FRIT glass is readily drawn into fibers using an up-draw process. The resulting fibers are chemically more durable than the original slag material. The hardness (and probably elastic modulus) of the FRIT glass is higher than E-glass and basalt, and the durability is reasonable.

- Compositional analysis of the FRIT indicated that it is higher in Si, Al and Fe, and lower in Ca than commercial basalt glass. The susceptibility of the slag to "foaming" during melting is due to excessive dissolved gases. These can be released at lower temperatures through pre-treatment to vitrify and cast or fiberize the molten glass at higher temperatures. It is possible, however, that the spontaneous foaming of the slag may be an advantage for some applications.

- The IGCC FRIT glass absorbs microwaves efficiently and the samples can be melted by microwave heating within minutes.

- FTIR studies on the emitted gases indicated the presence of CO, CO2, sulfur compound gases in the temperature range tested of up to 1000 deg C.

## *6.2 Utilization Potential for Novel Materials*

The use of FRIT mixed with inorganic pigments for glazes and enamels was considered after characterizing their physical and chemical characteristics in this study. Although there may be some highly specialized niches for the IGCC FRIT in such applications, it was concluded that byproduct FRIT may not be usable in the usual or traditional areas of inorganic pigments. First of all, such frits must be exceedingly uniform in properties, and the properties must be tailored for viscosity and thermal expansion. The FRIT is already heavily fluxed with lead and borates to lower the melting points. Even if we could take the hot slag and flux it directly to save energy, the color of the FRIT will still be a problem.

The project team believes that it is the refractory nature of this FRIT that we should utilize for development of beneficial uses. One application that could be that developed is that FRIT can be bonded to (not melted onto) the steel beams and girders in large buildings. In a fire, the heat will soften and melt and bond and may be even foam the FRIT, and thereby insulate the metal itself from softening and buckling. This could add another 30-60 minutes of time before the beams buckle. Fireproof glazing using FRIT can be very advantageous if it is cheap enough to implement. This might be a way to make this idea (suggested in the past and pursued by Corning with a “too expensive” synthetic material) a reality.

Microwave melting results revealed by accident that we could reduce the Fe-oxide to generate nano-metallic particles in the glass. If we do so with the spheres, they could be "magnetically" controlled to facilitate "fluid flow" or to target their trajectory. Some of the other applications could be low-weight filler, fluidized bed media to replace currently used synthetic ceramics that are more costly.

The foamed FRIT with good hardness properties and dark color may have potential for use as substrate for solar or other heat collection systems. Synthesis of available characterization data for byproduct FRIT suggests that it may have potential for use as an obscurance material for defense applications.

## *6.3 __Recommendations__*

The project team believes that additional focused studies should be performed to develop materials from byproduct FRIT that represent new markets for medium to large volume utilization. The following materials represent our best thinking at the present time.

- Fireproof glazing materials for steel structures
- Obscurance materials for defense applications.
- Substrate for solar or other heat collection systems.
- Spray insulation material for the building industry.
- Decorative tiles for the inside/ outside of buildings

During this study, the investigators focused on identifying suitable materials for further development. Minimal effort was expended in considering economic feasibility of these products since technical feasibility of these products needs to be established first. Future studies should consider economic feasibility studies as technical feasibility and process development studies are completed.

## 7.0 REFERENCES

Choudhary V, S. Kwan, Steve Hadley, (2000), Utilization of lightweight materials made from coal gasification slags, Final Report to U.S. Department of Energy, Cooperative Agreement DE-FC21-94MC30056

Chugh, Y.P., A. Pawardhan (2002), Development of Physical processing Techniques for Reduction of Loss on Ignition in Gasification Byproducts, Report to TECO Energy Plant, Mining and Mineral Resources Engineering, Southern Illinois University, (Confidential)

Charah Environmental, Inc ( Madisonville, KY), 2003, Private Communication

Conzone, S, R. Brown, D. Day, G. Ehrhardt (2002) "In-vitro and in-vivo dissolution behavior of a dysprosium lithium borate glass designed for the radiation synovectomy treatment of rheumatoid arthritis", Journal of biomedical materials research, 60 (2) p260-268

Norton, Olin ( 2004), Private Communication.

Norton, O, Ronald palmer, W. Gene Ramsey (2006), 'Enhancement of structural foam materials by incorporation of gasifier slag', Final report to National Energy Technology Laboratory, pp 52, March

Spiridonov, Yu. A., L.A. Orlova, D. I. Mendeleev (2003) Russian Chemical Engineering University, Moscow, Russia Glass and Ceramics, (Translation of Steklo iKeramika), 60(9-10), 313-314.

Norton, Olin, Ronald A. Palmer, and W. Gene Ramsey (2005)," Enhancement of Structural Foam Materials By Incorporation of Gasified Slag," Final report to National Energy Technology Laboratory, Cooperative Agreement DE-FC26-04NT42204, March 2005.